SVERIGES GEOLOGISKA UNDERSÖKNING

SERIE C NR 798 AVHANDLINGAR OCH UPPSATSER ÅRSBOK 76 NR 11

J. S. STUCKLESS B. TROËNG C. E. HEDGE
I. T. NKOMO K. R. SIMMONS

AGE OF URANIUM MINERALIZATION AT LILLJUTHATTEN IN SWEDEN

AND CONSTRAINTS ON ORE GENESIS

UPPSALA 1982

SVERIGES GEOLOGISKA UNDERSÖKNING

SERIE C NR 798 AVHANDLINGAR OCH UPPSATSER ÅRSBOK 76 NR 11

J. S. STUCKLESS B. TROËNG C. E. HEDGE
I. T. NKOMO K. R. SIMMONS

AGE OF URANIUM MINERALIZATION AT LILLJUTHATTEN IN SWEDEN

AND CONSTRAINTS ON ORE GENESIS

UPPSALA 1982

ISBN 91-7158-277-0
ISSN 0082-0024

Kartorna är godkända ur sekretessynpunkt för spridning.
Statens lantmäteriverk 1982-12-30.

Addresses:
J. S. Stuckless, C. E. Hedge,
I. T. Nkomo and K. R. Simmons
U.S. Geological Survey, Box 25046,
MS 963, Denver Federal Center,
Denver, CO 80225, U.S.A.

B. Troëng
Geological Survey of Sweden
Box 801
S-951 28, Luleå

Schmidts Boktryckeri AB
Helsingborg 1982

CONTENTS

ABSTRACT

Geologic, petrographic, geochemical, and isotopic studies have been combined to examine the genesis of the uranium ore deposit of Lilljuthatten, western Jämtland, Sweden, and its relationship to the Olden Granite. The complex geologic history of the area precludes unique interpretation of much of the data, but internally consistent and geologically reasonable models can be developed that suggest that similar ore deposits might reasonably be found elsewhere.

Analyses of six mineralized and four non mineralized whole-rock drill-core samples from the uranium deposit at Lilljuthatten yield a lead-lead isochron age of 420 ± 3 Ma. This age corresponds to the last stage of the Caledonian orogeny which indicates that the ore deposit most likely formed as a result of this event.

None of the isotopic systems examined have completely retained the intrusive age of the Olden Granite, but data for the Rb-Sr whole-rock, Pb-Pb whole-rock, and Pb-Pb galena and feldspar systems all suggest an age of approximately 1 650 Ma. There is a general correspondence between samples that exhibit open-system behaviour isotopically and samples that are displaced from the polybaric minimum in the system Q-Ab-Or. This indicates that Caledonian hydrothermal activity strongly affected most of the Olden Granite. Only oxygen isotope values, rare-earth-element contents and possibly thorium contents appear to have been unaffected by this event in all samples.

A model for the genesis of the ore deposit is proposed as follows: (1) derivation of a highly evolved granite by partial melting of crustal materials at 1 650 Ma ago; (2) pervasive hydrothermal alteration and fracturing of the granite in response to the Caledonian orogeny at approximately 420 Ma ago with mobilization of uranium and lead and precipitation of these elements in open fractures; and (3) recent modification of the Caledonian uranium distribution in response to exposure to near-surface conditions.

INTRODUCTION

The study of the Olden Granite and the uranium deposit at Lilljuthatten was initiated as part of the NEA/IAEA co-ordinated research and development project on uranium in granites. The objectives are to describe and to determine the age of the uranium mineralization at Lilljuthatten, Sweden, and to place constraints on ore genesis through petrologic, geochemical, and isotopic investigations.

The Olden Granite crops out in the northeastern part of the Olden Window within the central Scandinavian Caledonides (Fig. 1). The granite intrudes a supracrustal formation dominated by terrestrial metavolcanics (mainly rhyolitic in composition), and it also appears to intrude an extensive microgranite in the eastern part of the window (Fig. 2). Thin aplitic and dacitic dykes of unknown age cut the granite in a few places. Locally, the granite exhibits a weak foliation that may be interpreted as a primary magmatic flow foliation or as caused by a pre-Caledonian tectonic event.

The volcanic rocks and granites of the Olden Window are extensively intruded by gabbro-dolerites that have been geochemically compared (Johansson 1980) with the Central Scandinavian Group (Gorbatschev *et al.* 1979) of the autochthon. The latter have been dated by Patchett (1978) to approximately 1 200 Ma. Some of the early foliation of the granites may pre-date the intrusion of these basic dykes.

Sediments were deposited over the area from late Precambrian to Ordovician time. These are now preserved as a thin, discontinuous, and tectonically disturbed sequence of quartzite, black shale, limestone, and greywacke. Primary sedimentary contacts, demarcated by a thin conglomeratic horizon have been described along the eastern margin of the granite (Asklund 1938; Walser 1980).

Extensive thrusting towards the east took place in late Silurian time, and a strong cataclastic imprint was imposed on the Olden Granite coeval with a recrystallization under greenschist facies conditions (Harrison 1979). At least four different deformational episodes have been recognized in conjunction with the Caledonian overthrusting (Troëng 1982). After emplacement of the nappes, large late-stage antiforms were elevated which are now expressed as Precambrian basement in a number of windows along the Swedish-Norwegian border (Fig. 1). This late stage of deformation is characterized in the Olden area by subvertical fracture zones and faults, some of which are associated with uranium mineralization.

Earlier investigations of the Olden area have concentrated on the contact relations between the Proterozoic basement and the Phanerozoic sedimentary rocks at the eastern margin of the window (Törnebohm 1872, 1896; Frödin 1916; Asklund 1938, 1960). The amount of involvement of the Olden basement in the Caledonian thrusting is controversial and still remains to be solved. Thus the Olden anticline has been suggested to be allochthonous (Asklund 1938), autochthonous (Stephansson 1976), and parautochthonous (Gee and Zachrisson 1979).

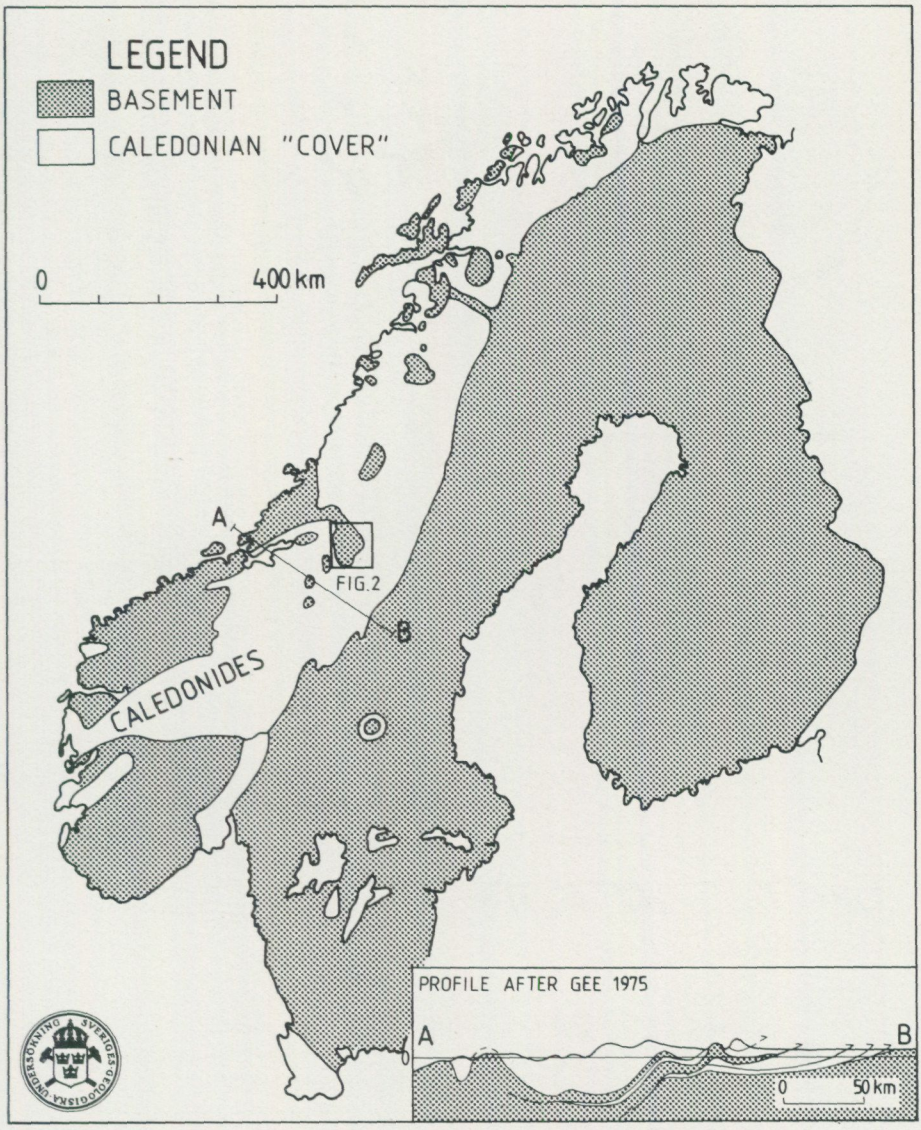

Fig. 1. Generalized geologic map of Scandinavia showing the location of the Olden Window and a generalized cross-section of the Caledonides (after Gee 1975).

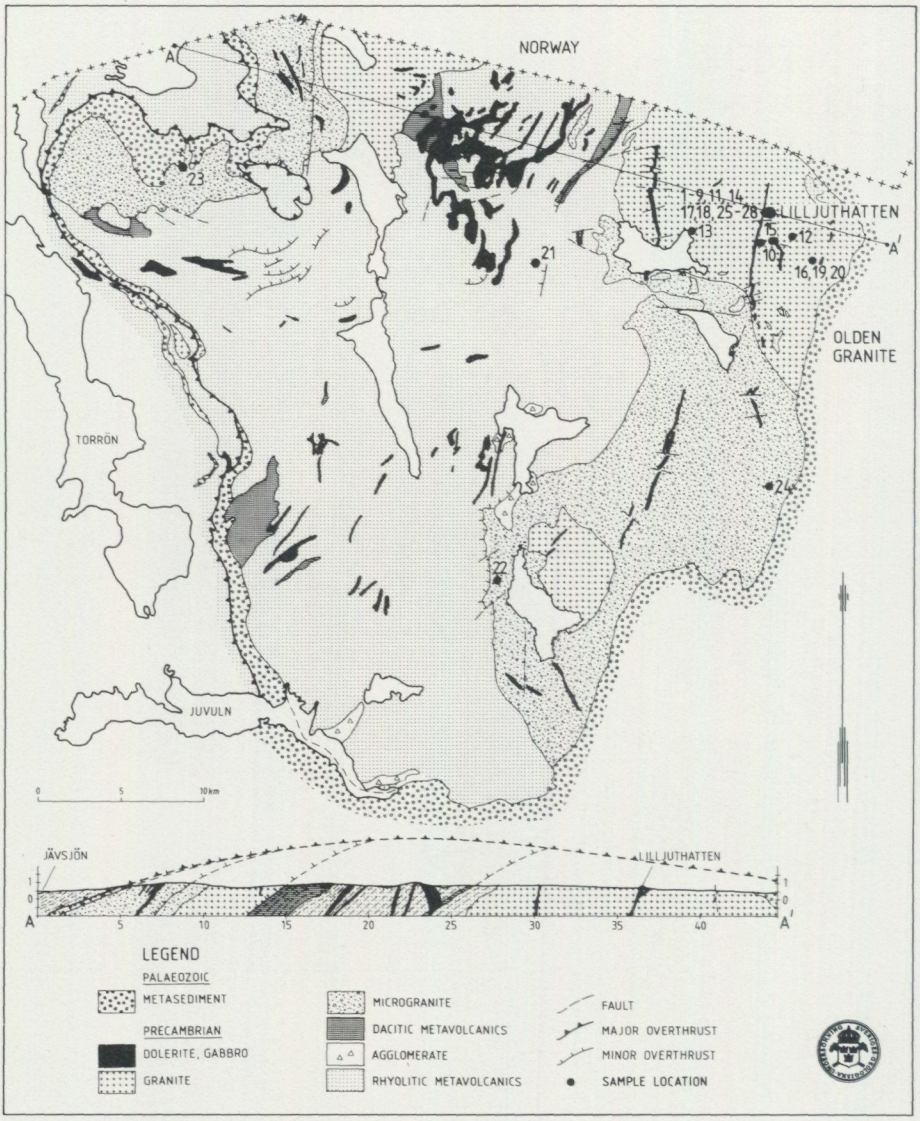

Fig. 2. Geologic map of the Olden Window showing sample locations.

The present authors are of the opinion that the basement is parautochthonous.

More recent investigations have concentrated on the Olden Granite and associated uranium mineralizations (Troëng and Wilson 1979; Klingspor and Troëng 1980; Troëng 1982). These studies have shown that the Olden Granite is a true granite by the classification of Streckeisen (1973) and that it is highly evolved as compared to an average granite of Taylor (1964).

Geochronologic studies (Klingspor and Troëng 1980) by the Rb-Sr whole-rock and mineral techniques and K-Ar whole-rock and mineral techniques failed to yield precise age information owing to the intensity of the Caledonian event. Seven Rb-Sr whole-rock analyses scatter about a reference isochron of 1 500 Ma for which an initial $^{87}Sr/^{86}Sr$ ratio of 0.7134 was calculated. K-Ar ages for plagioclase, biotite and potassium feldspar were determined to be 791 ± 6 418 ± 3, and 182 ± 1 Ma respectively. Of these ages, only the biotite age is thought to be meaningful. K-Ar biotite-ages date the last decrease in temperature to below that required for argon retention. Inasmuch as this temperature is approximately the same as that calculated by Harrison (1979) for metamorphic temperatures within the Olden window (~350°C by garnet-biotite geothermometry), 418 Ma probably approximates the end of the Caledonian event.

ANALYTICAL METHODS

URANIUM, THORIUM, AND LEAD ANALYSES

Uranium, thorium, and lead concentrations and the isotopic composition of lead were determined for 19 whole-rock samples (Table 1) and a potassium feldspar, fluorite, and four fractions of zircon (Table 2) by isotope dilution and mass spectrometry. In addition, the isotopic composition for four galenas was determined (Table 3). Six whole-rock samples were analyzed as partial or complete duplicates, and mean values for these samples are used in plots and computations. All analyses were made on a 12-inch NBS mass spectrometer.

All of the whole-rock samples and minerals were analyzed by a single dissolution technique followed by liquid aliquoting. This procedure minimizes sample-splitting errors and therefore increases the precision of parent-daughter isotopic ratios. All mass spectrometry for lead compositions and concentrations was accomplished by use of the silica gel-H_3PO_4 technique with zircon and fluorite data obtained with a single rhenium filament and whole-rock and feldspar data obtained with a triple rhenium filament mode.

Table 1. Uranium, thorium and lead concentrations and isotopic composition of lead for whole-rock and feldspar samples from the Olden Granite, Sweden

Sample number	U (ppm)	Th (ppm)	Pb (ppm)	$^{206}Pb/^{204}Pb$	$^{207}Pb/^{204}Pb$	$^{208}Pb/^{204}Pb$	Plot I.D.
77660	360.0	41.13	45.8	77.893	18.974	38.527	1
77662	10150	40.70	740.0	1500.9	97.549	38.563	
	10197	42.27	739.8	1513.7	98.206	38.613	
ave	10173	41.49	739.9	1507.3	97.878	38.588	2
77666	431.5	45.28	38.71	120.39	21.352	39.811	
	--	--	--	119.93	21.309	39.854	
ave	431.5	45.28	38.71	120.16	21.331	39.833	3
77735	1878	46.05	138.2	428.18	38.315	39.735	
	--	--	--	426.99	38.323	39.869	
ave	1878	46.05	138.2	427.59	38.319	39.802	4
77738	15316	56.28	1044	2543.2	155.08	40.961	
	15696	57.79	1072	2597.5	157.98	40.717	
ave	15496	57.03	1058	2570.4	156.53	40.839	5
77968	27.39	35.19	27.04	22.729	15.915	38.418	6
77972	48.49	47.96	25.58	27.520	16.190	39.359	7
77979	49.11	58.20	21.58	27.792	16.235	40.796	8
77981	16.70	36.79	29.77	23.338	15.978	38.386	
	--	--	--	23.336	15.968	38.357	
ave	16.70	36.79	29.77	23.337	15.974	38.372	9
79061	26.20	42.21	19.36	24.478	16.059	39.936	
	--	--	--	24.450	16.051	39.931	
ave	26.20	42.21	19.36	24.464	16.055	39.934	10
79911	1796	45.25	144.0	341.46	33.597	38.852	11
76032	17.71	58.69	29.39	25.038	16.190	41.374	12
76285	4.74	19.13	18.19	23.174	16.080	40.216	13
77988	16.87	46.2	39.51	25.017	16.259	40.947	14
79062	26.93	39.63	47.4	28.452	16.628	41.292	15
79070	17.83	88.65	35.59	27.861	16.496	44.555	16
79903	16.84	48.32	12.2	32.332	16.698	44.704	17
79914	27.39	101.7	37.57	35.248	17.187	44.723	
	26.75	101.9	36.08	35.225	17.175	44.767	
ave	27.07	101.8	36.33	35.237	17.181	44.745	18
Lill-1 WR	15.08	80.28	32.94	28.691	16.632	45.462	19
Lill-1 K'spar	0.44	0.17	33.67	18.746	15.701	37.517	20

Table 2. Uranium, thorium and lead concentrations and isotopic composition of lead for zircons and fluorite from sample Lill-1, Olden Granite, Sweden

Sample name	U (ppm)	Th (ppm)	Pb (ppm)	$^{206}Pb/^{204}Pb$	$^{207}Pb/^{204}Pb$	$^{208}Pb/^{204}Pb$
zr-1 -200 mesh non-mag	3124	1385	385.26	517.16	57.580	115.85
zr-2 -200 mesh mag	3897	1915	318.09	292.61	35.128	76.367
zr-3 +100 mesh black, non-mag	1568	631.0	191.61	302.52	38.732	85.610
zr-4 +100 mesh yellow, non-mag	4003	1866	391.79	511.28	54.422	107.86
fl-1	0.931	2.664	1.135	35.417	17.268	49.480

Zircon analyses were made using 1 to 6 mg of material and methods as described by Ludwig and others (1981). Approximately 40 mg of fluorite was hand picked to be free of visible impurities and analyzed in a manner similar to the zircons. Analytical uncertainties for zircon and fluorite data were calculated according to the methods of Ludwig (1980).

Whole-rock analyses were made on approximately 1-g splits of finely-pulverized rock. Chemical procedures are generally the same as described by Tatsumoto and others (1972) except that final purification of lead was accomplished by electroplating (Barnes and others 1973) purification of galena lead was done entirely by electroplating. Whole-rock and galena lead isotopic compositions are precise to 0.1% (2σ) and reported concentrations are precise to 0.2% (2σ).

Table 3. Lead-isotope compositions of galenas from the Olden Window, Sweden

Sample number	$^{206}Pb/^{204}Pb$	$^{207}Pb/^{204}Pb$	$^{208}Pb/^{204}Pb$	Plot I.D.
7783-023	16.381	15.393	35.720	21
78-313	21.727	16.001	39.758	22
78-026	22.581	16.138	40.674	23
79-240	23.799	16.198	40.615	24

RUBIDIUM AND STRONTIUM ANALYSES

Rubidium and strontium determinations were made, for 13 whole-rock samples (Table 4) with tracers of ^{87}Rb and ^{84}Sr. Samples were analyzed using triple rhenium filaments and a NBS 6-inch radius mass spectrometer. This mass spectrometer yields a value of 0.70802 ± 0.00006 (2σ) for the E and A $SrCO_3$ standard. All $^{87}Sr/^{86}Sr$ ratios are normalized to an $^{86}Sr/^{88}Sr$ ratio of 0.1194.

Analytical precision of rubidium and strontium concentrations and compositions is about the same as that reported for uranium and lead. However, for most samples, separate dissolutions were used for composition and concentration analyses. Replicate analyses for granitic samples indicates an analytical accuracy of ± 1.0 per cent for concentrations and ±0.03 per cent for isotopic composition (2σ). These errors are used for data regressions because they include splitting errors which can be highly significant for granitic materials.

Table 4. Rubidium, strontium, and $^{87}Sr/^{86}Sr$ ratio data for whole-rock samples from the Olden Granite, Sweden

Sample	Rb (ppm)	Sr (ppm)	$^{87}Sr/^{86}Sr$	$^{87}Sr/^{86}Sr$	Plot I.D.
79061	463.3	28.8	52.19	1.9402	10
79062	524.8	25.4	69.43	2.3568	15
79070	301.2	24.4	38.75	1.5719	16
79903	191.2	66.3	8.539	0.9464	17
79911	900.0	24.7	24.05	1.2282	11
79912	598.3	73.6	24.73	1.2209	25
79914	566.3	45.7	38.49	1.4465	18
79917	649.2	42.0	47.23	1.2659	26
76032	290.5	35.1	25.37	1.3038	12
76285	190.2	217.1	2.551	0.76995	13
77968	559.8	55.6	32.21	1.4422	6
77988	436.1	56.8	23.35	1.2282	14
Lill-1	282.9	23.2	38.20	1.5633	19

REGRESSION PROCEDURES AND AGE DETERMINATIONS

The determination of best fit lines for isochrons was made using the methods of York (1969). Secondary-isochron-age calculations were made using the formula of Rosholt and others (1973). Isotopic and decay constants used are those recommended by the IUGS Subcommission on Geochronology (Steiger and Jäger 1977; $\lambda(^{238}U) = 0.155125 \times 10^{-9}yr^{-1}$; $\lambda(^{235}U) = 0.98485 \times 10^{-9}yr^{-1}$; $\lambda(^{232}Th) = 0.049475 \times 10^{-9}yr^{-1}$; $\lambda(^{87}Rb) = 1.42 \times 10^{-11}yr^{-1}$; $^{238}U/^{235}U = 138.88$; and $^{85}Rb/^{87}Rb = 2.59265$).

CHEMICAL PROCEDURES

All but one of the samples (Lill-1) used in this study were analyzed by the Geological Survey of Sweden using X-ray fluorescence on lithium-tetraborate-fused samples for SiO_2, TiO_2, Al_2O_3, total iron as Fe_2O_3, MnO, CaO, MgO, K_2O, and BaO. P_2O_5 was determined colorimetrically. S, H_2O, and CO_2 were determined gravimetrically, and FeO was obtained by titration. Na_2O was determined by flame emission, and F by ion specific electrode. All but two samples (76032 and 76285) were analyzed by the U.S. Geological Survey by high precision X-ray fluorescence (Taggart and others 1982). Statistical evaluation of the paired analyses shows no significant differences for major elements. However, in order to take advantage of the extra significant figure and high precision for several elements (± 2 per cent 2σ), the data reported in Table 5 were obtained by combining the two sets of data. Data for SiO_2, Al_2O_3, MgO, CaO, Na_2O, and K_2O for the replicated samples were obtained by XRF. The fourth digit reported for SiO_2 and Al_2O_3 is not significant for any specific sample but may carry significance for the average data set (A. T. Miesch, oral commun., 1981). Data for FeO, and Fe_2O_3 were obtained from the total Fe_2O_3 determined by XRF and partitioned according to the ferrous/ferric ratio determined by the Geological Survey of Sweden. All other data reported in Table 5 are from the determinations of the Geological Survey of Sweden. Normative minerals were computed using the program GNAP (Stuckless and VanTrump 1979).

Rare-earth-element concentrations (Table 6) were determined by instrumental neutron activation analysis using methods similar to those of Gordon and others (1968). Data for four samples (77660, 77662, 77735, and 77738) were obtained by INAA following radiochemical separation (Zielinski 1975) in order to avoid extreme interference from uranium. Raw data were adjusted within counting statistic errors to give the smoothest chondrite normalized patterns. Chondrite values in normalization of the data are those of Evensen and others (1978).

Table 5. Chemical and normative data for granitic samples from the Olden area, Sweden

	76032	76285	77660	77662	77666	77735	77738	77968	77972	77979	77981	77988
Plot I.D.[1]	12	13	1	2	3	4	5	6	7	8	9	14
SiO2	75.20	70.90	75.49	69.78	74.25	72.43	64.44	71.21	74.11	72.62	73.73	73.02
Al2O3	12.10	14.70	12.93	13.54	13.30	14.22	15.98	14.41	13.08	13.77	13.45	13.38
Fe2O3	0.30	1.30	0.32	1.34	0.39	1.00	0.61	0.43	0.20	0.11	0.10	0.11
FeO	1.10	1.60	0.75	1.15	0.97	0.27	1.92	0.87	1.17	1.49	1.21	1.58
MgO	0.15	0.75	0.29	0.85	0.28	0.36	0.79	0.15	0.28	0.29	0.17	0.21
CaO	0.40	1.80	0.26	0.38	0.31	0.62	0.66	0.70	0.70	0.64	0.77	0.97
Na2O	3.40	4.00	3.50	2.93	3.49	3.70	3.53	3.38	3.39	3.49	3.59	3.44
K2O	4.90	4.50	5.18	5.66	5.30	5.86	6.78	6.61	5.13	5.64	5.34	5.25
H2O	0.50	0.90	0.40	0.80	0.35	0.50	0.80	0.45	0.55	0.35	0.45	0.55
TiO2	0.01	0.33	0.13	0.14	0.15	0.13	0.16	0.11	0.13	0.15	0.11	0.16
P2O5	0.01	0.10	0.05	0.07	0.05	0.06	0.08	0.05	0.06	0.06	0.04	0.07
MnO	0.03	0.09	0.04	0.04	0.04	0.04	0.06	0.04	0.04	0.05	0.05	0.06
CO2												
F	0.02	0.03	0.05	0.06	0.05	0.25	0.25	0.33	0.36	0.27	0.35	0.37
BaO	0.03	0.07	0.06	0.03	0.06	0.06	0.07	0.07	0.05	0.06	0.06	0.07
TOTAL (-O)	98.14	101.06	99.43	96.74	98.97	99.40	96.02	98.67	99.10	98.88	99.27	99.08
NORMATIVE MINERALS												
Q	35.491	24.792	34.310	29.928	32.574	27.681	15.622	25.467	33.557	29.084	30.962	30.893
C	0.541	0.223	1.302	2.269	1.476	1.432	2.532	1.388	1.756	1.592	1.360	1.385
OR	29.504	26.313	30.786	34.572	31.645	34.839	41.723	39.586	30.590	33.707	31.787	31.310
AB	29.315	33.493	29.786	25.627	29.839	31.499	31.106	28.986	28.946	29.867	30.600	29.377
AN	1.863	8.163	0.743	1.125	0.997	1.007	1.146	0.901	0.580	0.965	1.139	1.835
EN	0.381	1.848	0.726	2.188	0.705	0.902	2.049	0.379	0.704	0.730	0.426	0.528
FS	1.846	1.471	0.978	0.876	1.299		2.988	1.150	1.860	2.519	2.066	2.682
FO												
FA												
MT	0.433	1.865	0.467	2.008	0.571	0.628	0.921	0.632	0.293	0.161	0.146	0.161
HM						0.573						
IL	0.019	0.620	0.248	0.275	0.288	0.248	0.316	0.212	0.249	0.288	0.210	0.307
RU												
AP	0.024	0.234	0.119	0.171	0.120	0.143	0.197	0.120	0.143	0.144	0.095	0.167
FR	0.040	0.043	0.094	0.114	0.095	0.506	0.520	0.678	0.735	0.550	0.717	0.754
CC												
TOTAL	99.471	99.067	99.560	99.154	99.608	99.459	99.121	99.499	99.413	99.608	99.509	99.400
SALIC	96.718	92.985	96.927	93.521	96.531	96.459	92.130	96.329	95.429	95.215	95.847	94.801
FEMIC	2.753	6.082	2.633	5.633	3.077	3.000	6.991	3.171	3.984	4.392	3.661	4.600
D.I.[2]	94.309	84.598	94.882	90.127	94.058	94.019	88.452	94.039	93.093	92.658	93.348	91.581
USER DEFINED VARABLES												
PERAL[3]	1.041	0.998	1.092	1.164	1.105	1.049	1.114	1.030	1.055	1.058	1.028	1.021
PERAK[4]	1.110	1.284	1.138	1.237	1.159	1.144	1.216	1.133	1.175	1.162	1.151	1.180

Uranium and thorium concentrations were determined for eleven samples by both delayed neutron analysis (Millard 1976) and by gamma-ray spectrometry (Bunker and Bush 1966, 1967). Results for both of these techniques are generally precise to ±3 per cent of the amount reported (Table 7), and because of the relatively large sample sizes (7 and 600 g, respectively) and consequent small splitting errors, the accuracy is expected to be about the same as the precision.

MICROPROBE ANALYSIS

The microprobe analyses were carried out at the Mineralogy Division of the Institute of Geological Sciences, London. The equipment used was a Cambridge Instruments Microscan 5 fitted with an ED facility. The ED detector allowed simultaneous measurement of the elements: Ti, Mn, Fe, Ta, Nb, Y, Pb, Th, U,

Table 5. Chemical and normative data for granitic samples from the Olden area. Sweden--continued

	79061	79062	79070	79901	79903	79906	79908	79911	79912	79914	79917	Lill-1
Plot I.D.[1]	10	15	16	27	17	28	29	11	25	18	26	19
SiO2	76.93	75.84	75.40	74.46	76.22	75.51	73.95	70.21	63.81	73.13	60.08	76.81
Al2O3	12.55	12.57	12.64	13.13	13.05	12.91	13.39	14.61	19.09	12.47	18.77	12.07
Fe2O3	0.30	0.68	0.21	0.10	0.19	0.21	0.53	1.02	0.52	0.62	0.86	1.80
FeO	0.79	0.46	1.03	1.15	0.19	1.16	1.16	1.23	1.25	2.49	3.53	
MgO	0.17	0.05	0.12	0.19	0.12	0.16	0.21	0.88	0.35	0.29	1.95	0.18
CaO	0.08	0.65	0.77	0.82	0.70	0.86	0.63	0.27	0.53	1.47	0.48	0.74
Na2O	3.79	3.75	3.37	3.52	4.57	3.52	3.61	3.33	5.33	3.39	3.99	3.26
K2O	4.37	4.53	5.24	5.16	4.14	4.89	5.39	6.23	7.87	4.24	8.35	4.81
H2O	0.30	0.40	0.45	0.40	0.20	0.50	0.60	0.80	0.50	0.60	1.20	0.13
TiO2	0.07	0.07	0.10	0.11	0.11	0.11	0.13	0.16	0.22	0.27	0.19	0.08
P2O5	0.01	0.02	0.01	0.03	0.02	0.03	0.03	0.04	0.04	0.05	0.05	0.02
MnO	0.02	0.03	0.02	0.03	0.01	0.02	0.02	0.03	0.02	0.06	0.08	0.01
CO2	0.01	0.01	0.03	0.06	0.20	0.02	0.01	0.03	0.04	0.02	0.18	
F	0.03	0.39	0.29	0.30	0.05	0.35	0.26	0.04	0.12	0.65	0.06	
BaO	0.02	0.02	0.01	0.04	0.06	0.03	0.06	0.05	0.08	0.02	0.08	
TOTAL (-O)	99.43	99.31	99.57	99.37	99.81	100.13	99.87	98.91	99.72	99.50	99.82	99.91
NORMATIVE MINERALS												
Q	37.571	36.673	34.357	32.694	32.873	34.583	30.891	25.102	0.861	34.301		37.677
C	1.561	1.425	0.891	1.253	0.380	1.291	1.219	2.151	1.291	1.524	2.933	0.204
OR	25.972	26.956	31.099	30.684	24.511	28.858	31.892	37.219	46.637	25.182	49.429	28.449
AB	32.255	31.953	28.640	29.973	38.744	29.746	30.586	28.487	45.228	28.830	33.822	27.610
AN	0.092	0.226	1.473	1.397	1.837	1.453	1.092	0.720	1.412	2.160	0.656	3.544
EN	0.426	0.125	0.300	0.476	0.299	0.398	0.524	2.216	0.874	0.726	3.393	0.449
FS	1.131	0.225	1.597	1.915	0.029	1.810	1.517	1.221	1.544	3.745	3.917	
FO											1.032	
FA											1.313	
MT	0.437	0.993	0.306	0.146	0.276	0.304	0.769	1.495	0.756	0.903	1.249	
HM												1.802
IL	0.134	0.134	0.191	0.210	0.209	0.209	0.247	0.307	0.419	0.515	0.361	0.021
RU												0.069
AP	0.024	0.048	0.024	0.072	0.047	0.071	0.071	0.096	0.095	0.119	0.119	0.047
FR	0.060	0.803	0.597	0.615	0.099	0.713	0.529	0.076	0.240	1.333	0.114	
CC	0.023	0.023	0.069	0.137	0.456	0.045	0.023	0.069	0.091	0.046	0.410	
TOTAL	99.686	99.584	99.542	99.572	99.762	99.482	99.361	99.159	99.448	99.384	98.748	99.871
SALIC	97.451	97.234	96.459	96.001	98.345	95.932	95.681	93.680	95.428	91.997	86.840	97.483
FEMIC	2.235	2.351	3.083	3.571	1.416	3.550	3.680	5.479	4.019	7.387	11.908	2.388
D.I.[2]	95.798	95.582	94.095	93.350	96.129	93.187	93.369	90.809	92.725	88.313	83.251	93.736
USER DEFINED VARIABLES												
PERAL[3]	1.130	1.026	1.002	1.020	0.983	1.021	1.037	1.149	1.046	0.971	1.139	1.013
PERAK[4]	1.145	1.135	1.127	1.154	1.088	1.165	1.137	1.195	1.104	1.227	1.203	1.142

[1] Plot I.D. is underscored for samples with biotitic alteration

[2] D.I. is the differentiation index of Thornton and Tuttle (1960).

[3] Peral is the molar ratio of Al_2O_3 to Na_2O plus K_2O plus CaO.

[4] Perak is the molar ratio of Al_2O_3 to Na_2O plus K_2O.

whilst in parallel two further elements (e.g. Ca, Si or Nb) were measured on the crystal spectrometers. The probe was operated at 35 KV and a 200 sec. counting time. Uranium was analyzed using a synthetic UO_2 crystal and Th using a synthetic glass (Smellie *et al.* 1978).

Correction of the raw data was made using the ZAF computer program of Mason *et al.* (1969), the final results are quoted as oxide fractions (Table 9). (Note: U is given as U_3O_8 but is present in non-determinable proportions as the two oxides UO_2 and UO_3.)

Table 6. Rare Earth element contents in parts per million for samples from the Olden Granite, Sweden

Sample Name	La	Ce	Nd	Sm	Eu	Gd	Tb	Dy	Tm	Yb	Lu
77660	39.61	81.40	39.17	9.39	0.350	9.48	1.80	13.29	1.73	11.95	1.88
77662	75.55	145.5	58.83	11.96	0.98	10.88	2.26	16.70	2.30	15.70	2.44
77666	52.80	99.85	45.70	9.65	0.399	8.96	1.67	11.97	1.58	10.90	1.66
77735	35.00	76.40	37.33	8.52	0.390	7.59	1.62	12.07	1.69	11.00	1.78
77738	82.58	170.4	76.70	17.0	1.84	15.9	2.93	21.55	2.85	19.40	3.08
77968	52.71	107.7	50.93	9.43	0.745	11.77	1.95	12.77	1.29	9.74	1.91
77972	58.29	131.8	63.76	13.09	0.599	13.54	2.4	15.52	1.75	12.67	2.63
77979	75.89	159.2	75.95	14.95	0.726	16.91	2.97	21.58	2.14	14.75	3.0
77981	49.10	98.78	50.43	10.32	0.648	12.02	2.16	15.47	1.62	12.03	2.48
77988	71.13	144.7	62.34	11.34	0.844	12.33	2.08	13.7	1.32	9.10	1.05
79061	13.3	38.74	22.71	5.62	0.296	7.84	1.38	--	1.28	10.72	1.96
79062	36.93	89.29	43.54	10.69	0.290	10.87	2.45	--	2.25	18.64	3.12
79070	50.79	106.6	49.41	9.73	0.272	9.15	1.33	7.83	0.78	5.93	0.88
79901	49.72	107.3	43.20	9.78	0.556	--	1.72	10.86	1.44	12.75	2.01
79903	45.73	104.0	47.15	10.14	0.580	10.3	1.82	11.78	1.56	12.83	2.05
79906	45.62	97.50	42.45	9.26	0.515	9.59	1.68	10.78	1.43	11.81	1.84
79908	54.86	113.5	46.31	9.76	0.640	--	1.71	10.21	1.37	11.32	1.75
79911	--	--	--	--	0.289	--	1.21	8.44	1.33	10.89	--
79912	86.55	190.4	73.67	14.24	0.674	13.27	2.19	13.12	1.89	15.26	2.35
79914	--	292.9	120.0	25.12	0.616	24.65	3.88	22.96	3.12	22.90	3.47
79917	56.94	125.0	52.22	8.78	0.647	8.70	1.21	7.55	1.03	8.40	1.39
Lill-1	48.74	104.0	45.4	8.65	.243	7.70	1.22	7.70	0.72	5.12	0.82

Table 7. Uranium and radium-equivalent uranium (RaeU) values for granitic samples from the Olden Granite area, Sweden

Sample Name	U (ppm)	RaeU (ppm)	Plot I.D.
79061	27.5	22.5	10
79062	26.5	26.4	15
79070	19.1	10.1	16
79901	22.4	18.6	27
79903	17.4	11.5	17
79906	20.4	19.2	28
79908	19.6	23.0	29
79911	1794	1640	11
79912	28.2	26.6	25
79914	28.6	22.1	18
79917	16.9	23.5	26

RESULTS AND DISCUSSION

PETROGRAPHY

The Olden Granite is a coarse- to medium-grained biotite granite that contains subequal amounts of quartz, plagioclase, and perthitic microcline. Mafic phases account for less than six per cent of the rock by volume and are dominated by biotite with subordinate amounts of chlorite, epidote, and allanite. Zircon, iron and titanium oxides, and fluorite are the most common accessory minerals. Other accessory minerals are shown on Figure 3. Porphyritic and poikilitic textures are common and although much of the granite has been affected by recrystallization, there is a suggestion that the original texture was hypidiomorphic granular.

Three stages (Fig. 3) have been recognized in the mineralogical history of the granite: a magmatic, a metamorphic, and a hydrothermal stage (Troëng 1982).

Stage I, the magmatic stage, is characterized by crystallization of the main rock components. Textural relations suggest that crystallization of potassium feldspar superseded that of plagioclase. This interpretation is complicated by the possibility of renewed growth of potassium feldspar during the metamorphic stage as shown by overgrowths of microcline on subhedral primary plagioclase. The paragenesis of the mafic and accessory minerals is difficult to decipher due to extensive recrystallization during the metamorphic event. These minerals are generally interstitial to the tectosilicates or poikilitic near the rims, and are therefore presumed to be paragenetically late. Although primary mafic phase contents are generally low, small, local aggregates of mainly biotite exist. These mafic aggregates contain abundant inclusions of zircon with subordinate allanite, monazite, uranothorite, and complex uranotitanates and uranotantalates. These assemblages are inferred to be late-stage magmatic segregates. To date, no primary uraninite has been found in the Olden Granite.

Stage II, the metamorphic stage, is presumed to be coeval with the Caledonian orogeny of Late Silurian time. At that time, numerous fracture zones and joints cut the granite. Feldspars developed numerous microfractures and bent twin lamallae. Quartz and biotite were partly to completely recrystallized and were locally remobilized into open structures. Towards the end of the metamorphic stage, muscovite replaced some of the secondary biotite.

Stage III, the hydrothermal stage, is characterized by fracture filling with quartz, chlorite, muscovite, fluorite, and small amounts of calcite. At Lilljuthatten, a much more intense hydrothermal alteration is obvious. This alteration predated mineralization and may have provided a major control for ore localization. This alteration is not conclusively related to the pervasive hydrothermal alteration that affected most of the Olden Granite, and it is therefore treated separately.

The most extreme examples of biotitic alteration are rocks of mafic composition within which rounded, remnant clasts of potassium feldspar occur in a fine-

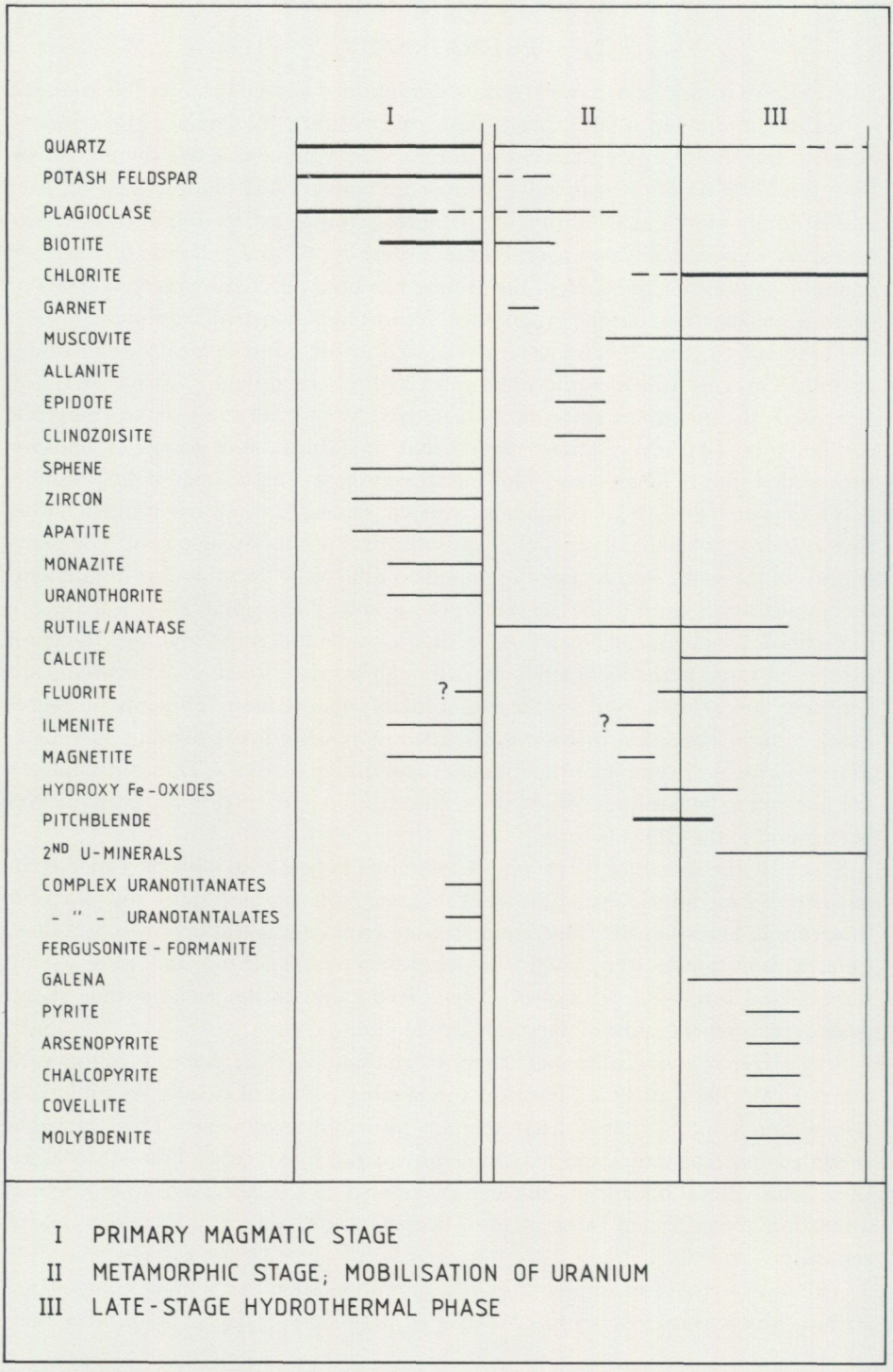

Fig. 3. Paragenetic scheme for the crystallization sequence of the Olden Granite. The relative mineral abudances is shown schematically by relative bar thicknesses (after Troëng 1982).

grained black matrix of secondary biotite (Fig. 4). The altered structures show all gradations from thin joints (Fig. 5) to fracture zones a couple of meters wide. The size of secondary biotite grains is generally about 0.05 mm. In-filling along fractures in potassium feldspars is common (Fig. 5). The differences in modal composition between normal and biotitically altered granite is given in Table 8. The biotite content of the altered rock is nearly ten times greater than in the normal granite. Quartz is markedly lower in the altered rock, and plagioclase is almost absent. There is no optical evidence for renewed growth of potassium feldspar; the apparent increase in potassium feldspar may therefore be an artifact caused by counting too few thin sections with large feldspar grains relative to the size of the area counted. The amounts of chlorite and muscovite are highly variable among the biotitically altered samples, and hence any systematic variation in the amounts of these minerals as a function of alteration cannot be evaluated with the available data.

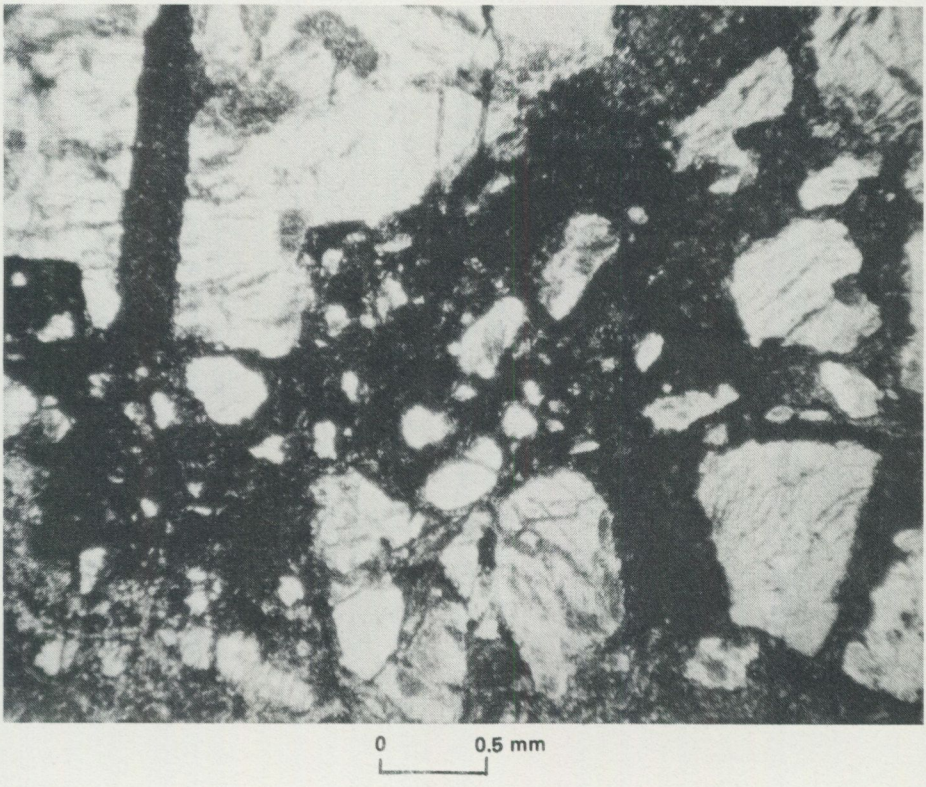

Fig. 4. Photomicrograph showing an extreme example of biotitic alteration.

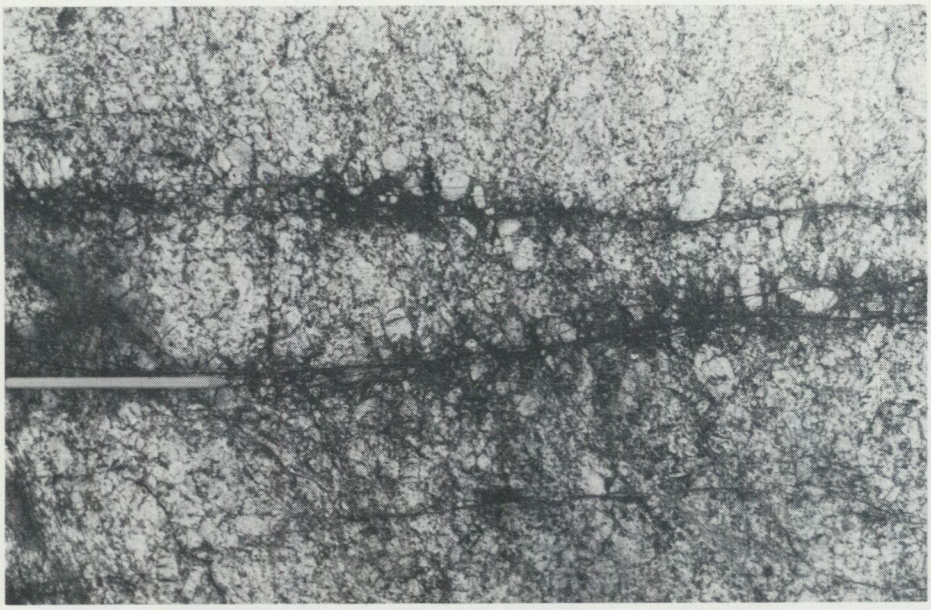

Fig. 5. Photograph showing biotitically altered and mineralized outcrop at Lilljuthatten, Sweden.

The uranium deposit at Lilljuthatten (Troëng and Wilson 1979; Troëng 1982) is located between two dolerite dykes (Fig. 6) within the coarse-grained central part of the Olden Granite and is generally localized in altered fracture zones (Fig. 5). The dominant trend of these zones is northeasterly and thus intersects the main dolerite at an oblique angle. The mineralization appears to be confined between

Table 8. Average modal compositions of biotitically altered and normal granite

	Normal granite	Altered granite
No. of samples	7	3
Quartz	36	10
K-feldspar	30	49
Plagioclase	28	0.1
Biotite	3.4	32
Muscovite	1.8	5.9
Chlorite	0.6	1.8
Acc	0.6	1.8

and perhaps controlled by the two dikes as nothing has been found below the dyke with a shallow dip and only minor showings occur on the western side of the major dike. However, the role of the dykes in ore formation is not clear. The dimensions of the mineralized body are approximately 225 by 100 by 50 m. The deposit is estimated to contain 2000 tons of uranium ore at an average grade of 0.14 per cent. The individual mineralized structures are irregular and vary from a couple of meters wide in well-developed fracture zones to very thin infillings of joints. Both extremes are generally associated with conspicuous mafic alteration (Fig. 7).

The mineralogy of the deposit is uncomplicated. The major identified uranium-bearing minerals are pitchblende, coffinite, and secondary uranium minerals. Pitchblende is the dominant uranium phase and occurs in botryoidal and spherulitic forms. No significant compositional differences have been detected between the textural forms of pitchblende. Alteration of the pitchblende is seen as areas of low reflectivity in connection with fractures on irregular patches within the grains (Fig. 8). Microprobe analyses of these altered parts show increases in silicon, iron, and calcium, and a decrease in uranium, cerium, and yttrium (Table 9). The data also indicate a primary variation in these elements, but this variation is much less than that caused by secondary alteration. The lead content is nearly constant which suggests that radiogenic lead has been immobile since the time of uranium deposition. However, rare galena crystals have been formed in fractures within pitchblende, but this again indicates immobility of radiogenic lead on the scale of a whole-rock sample. The colloform texture and low thorium content of the pitchblende both indicate that precipitation occurred at low temperatures.

Table 9. Microprobe analyses of altered and unaltered pitchblende from the deposit at Lilljuthatten, Sweden

(Data are in weight percent)

	Unaltered				Altered	
Sample	1	2	3	4	5	6
U_3O_8	88.8	87.2	87.5	81.4	69.7	70.4
ThO_2	0.4	0.9	0.5	0.4	0.5	0.8
PbO	5.4	4.4	5.2	4.3	3.2	3.9
SiO_2	0.1	0.1	0.2	3.6	5.4	3.9
CaO	1.6	1.7	1.5	2.6	2.4	2.8
FeO	0.2	0.1	0.1	4.8	3.9	7.2
Ce_2O_3	0.5	0.7	0.8	0.9	0.3	0.5
Y_2O_3	0.6	0.7	0.7	0.7	0.5	0.5
Total	97.6	95.8	96.5	98.7	85.8	90.0

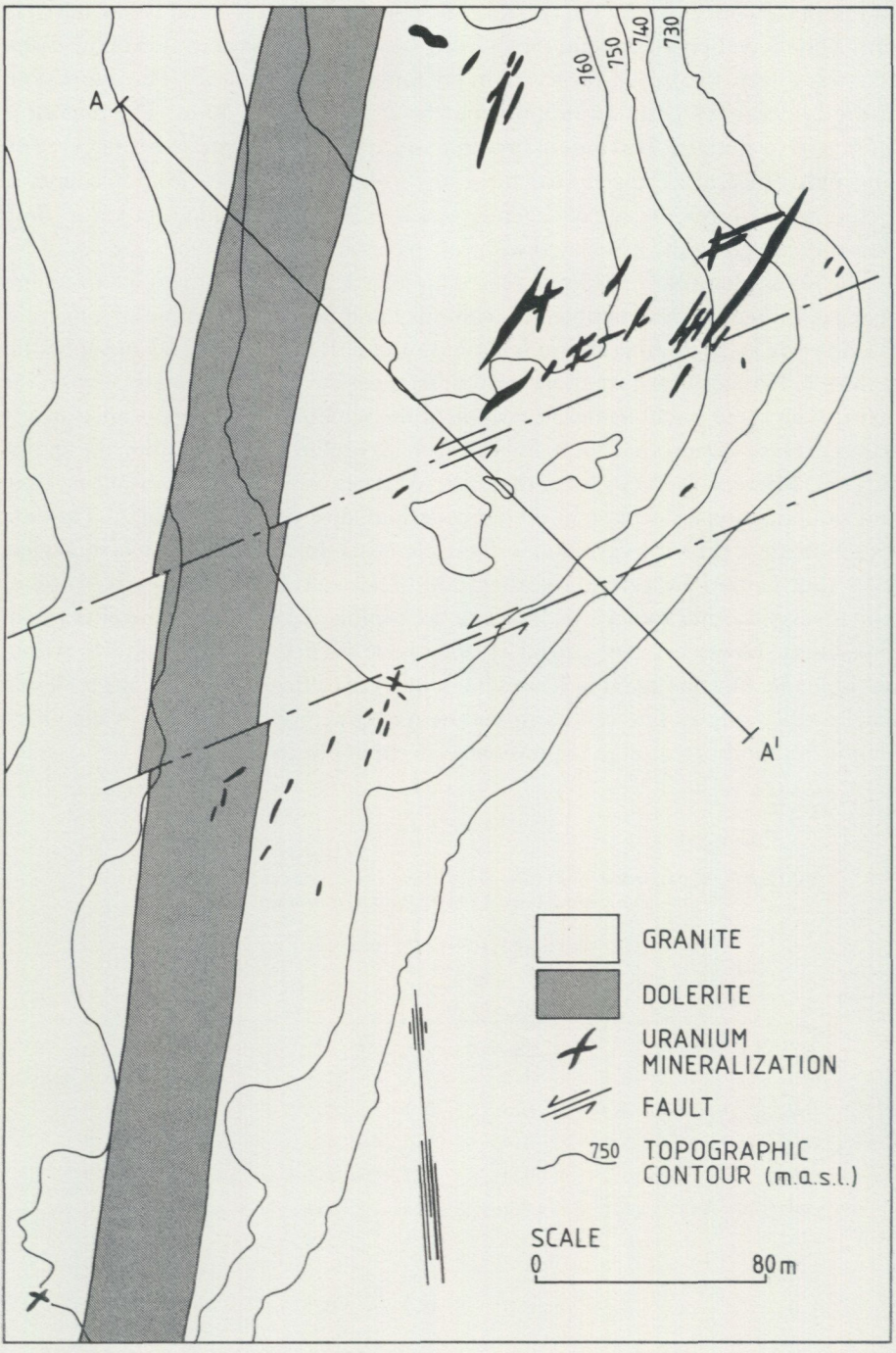
A
A'
760
750
740
730
GRANITE
DOLERITE
URANIUM MINERALIZATION
FAULT
750 TOPOGRAPHIC CONTOUR (m.a.s.l.)
SCALE
0
80 m

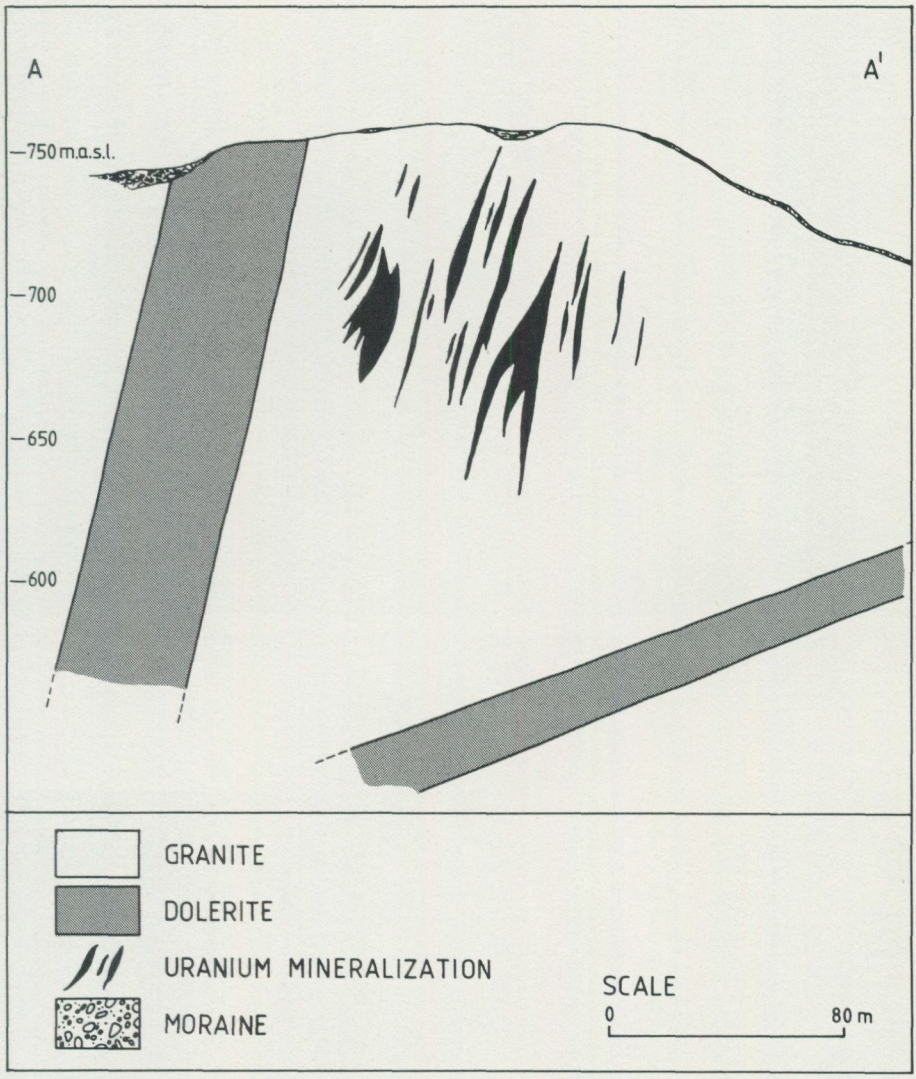

Fig. 6. Schematic map (left) and cross-section (above) showing the relationship of mineralization to dolerite dikes.

Fig. 7. Photomicrograph showing pitchblende veins in biotitically altered granite at Lilljuthatten, Sweden.

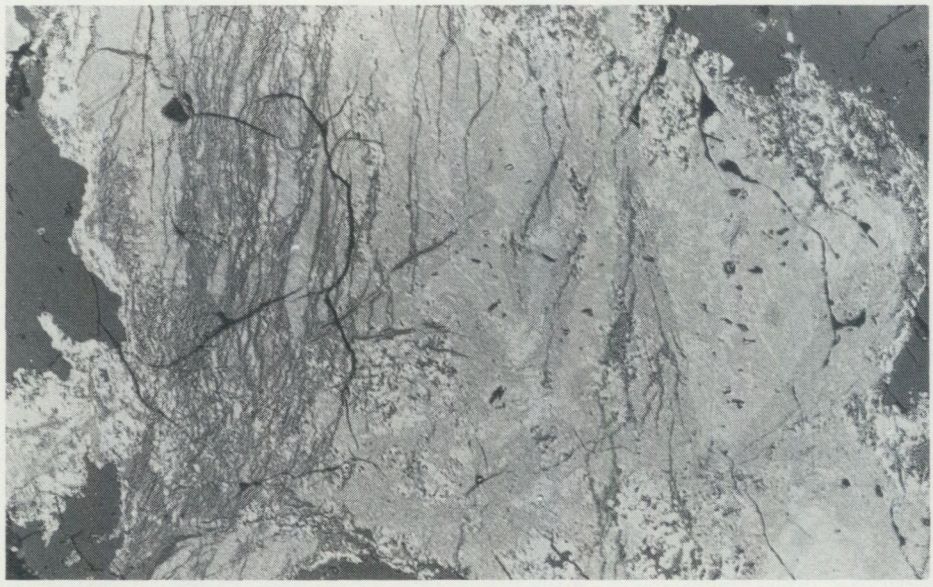

Fig. 8. Photomicrograph showing fresh and altered pitchblende from the deposit at Lilljuthatten, Sweden.

CHEMISTRY AND PETROLOGY

The major-element composition of the unaltered granites is fairly uniform (Troëng 1982) and exhibits several similarities to features of highly evolved granites (Table 5). Silica content for eighteen apparently unaltered granites is greater than 70.0 weight per cent, and CaO is less than one per cent for all but two samples. The potassium content generally exceeds that of sodium with K_2O generally greater than 5.0 weight per cent. The homogeneous and evolved nature of the granite is documented best by the differentiation index of Thornton and Tuttle (1960) which ranges from 84.6 to 96.1, but is greater than 92.7 for all but three of eighteen samples (Table 5) and averages 93.1 ± 2.8.

The degree of alumina saturation is fairly low relative to many other highly evolved granites. All eighteen samples are corundum normative, but none contains more than 1.8 weight per cent (Table 5). The molar ratio of Al_2O_3 to Na_2O plus K_2O plus CaO is greater than one for all but three samples (Table 5, Fig. 9), but is greater than 1.1 for only three samples. Thus the granite suite as a whole is best classified as weakly peraluminous.

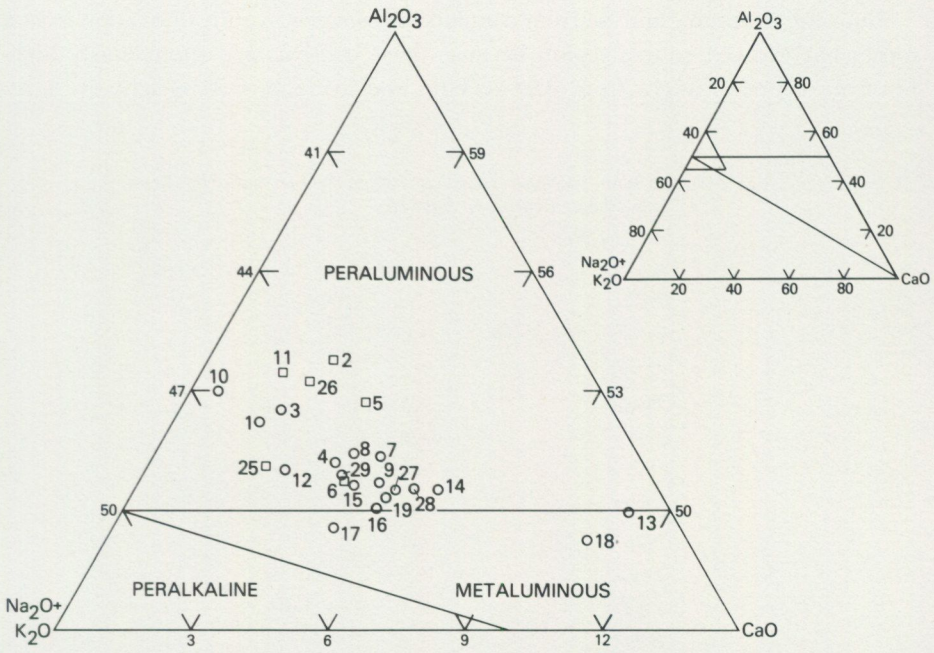

Fig. 9. Ternary diagram of molar alumina, sodium plus potassium oxide, and lime for granitic samples from the Olden Granite, Sweden, with fields for peraluminous, metaluminous, and peralkaline granites (after Shand 1951). Squares correspond to samples with biotitic alteration. Other samples are shown by circles. Numeric identification corresponds to symbol in Table 5.

Many peraluminous granites yield anomalously high $\delta^{18}O$ values (O'Neil and Chappell 1977; O'Neil and others 1977; Taylor 1968). Oxygen isotope data (provided by Dr. D. B. Wenner, University of Georgia) for eleven granite samples are not anomalously rich in ^{18}O (Table 10). The samples are similar to those from at least one other weakly peraluminous granite in both their large range and mean value (Wenner 1981). Both the oxygen isotope data and the low degree of alumina saturation suggest that the granite at Lilljuthatten did not have a large component of pelitic material in the source region that melted to form the granite.

Although the oxygen and some major element data do not suggest a highly evolved source region for the granite at Lilljuthatten, the rare-earth data (Fig. 10, Table 6) indicate that the source region was at least of continental affinity. All but one of the chondrite-normalized rare-earth patterns show lanthanum enrichment of greater than 100, and all of the patterns show a pronounced europium anomaly. These features are typical of crustally derived granites or granites that interacted strongly with crustal materials (Buma and others 1971; Barker and others 1976; Stuckless and Miesch 1981). The development of such strong enrichment of light rare-earth elements and pronounced europium anomalies from an unevolved source region would require unreasonably small degrees of partial melting and unreasonably large amounts of differentiation (Hanson 1978).

Fluorine, uranium, and thorium contents also suggest granite derivation from a somewhat evolved source region because these contents are anomalously high. Fluorine content ranges from 0.02 to 0.65 and averages 0.24 weight per cent.

Table 10. Oxygen isotope results for granitic samples from the Olden Granite, Sweden

Sample name	$\delta^{18}O$	Plot I.D.
77662	7.0	2
77735	7.6	4
77968	7.1	6
77972	8.0	7
77979	7.3	8
77988	6.7	14
79061	7.2	10
79062	7.3	15
79963	9.2	17
79911	7.8	11
79914	7.4	18

Data provided by Dr. D. B. Wenner, University of Georgia, and reported relative to SMOW.

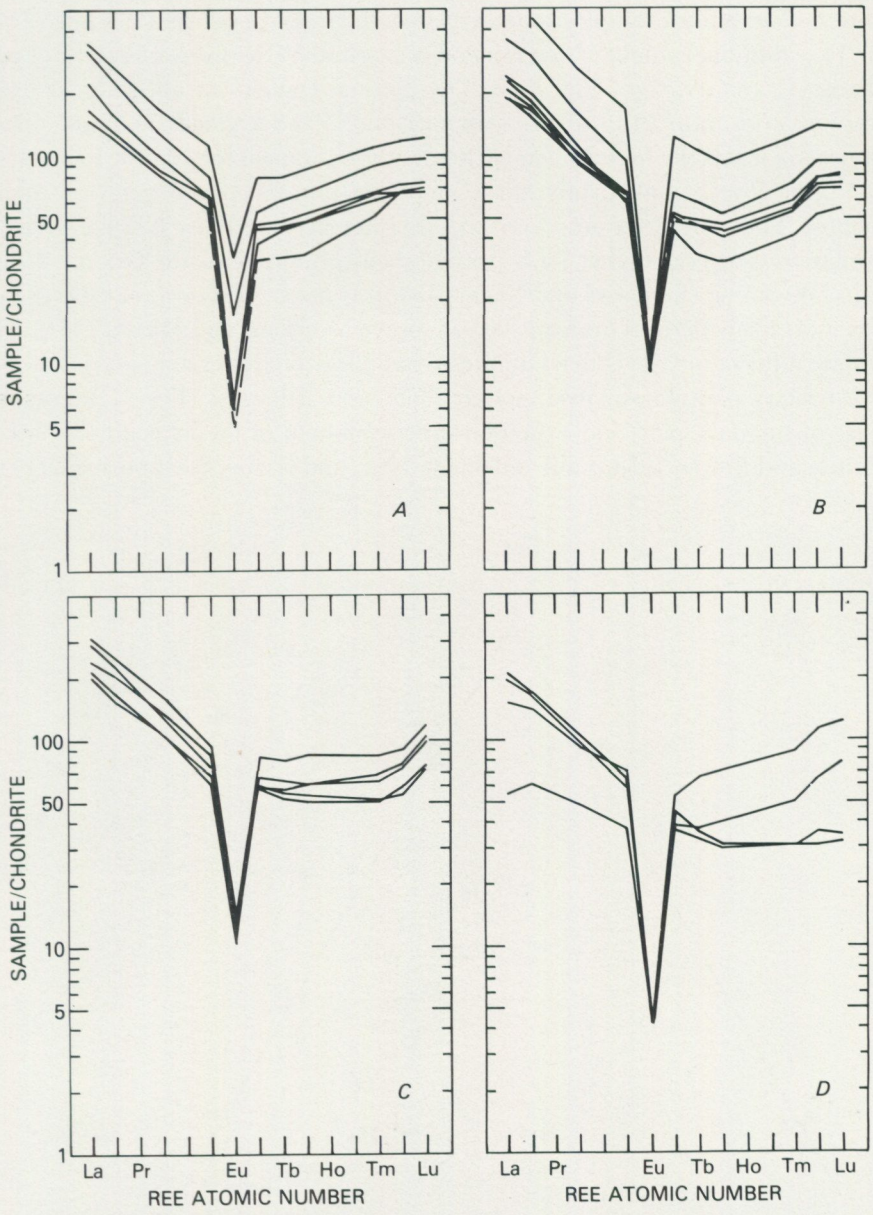

Fig. 10. Chondrite-normalized rare-earth patterns for granitic samples from the Olden Granite, Sweden. A is patterns for six mineralized granites; three with biotitic alteration and three without. B and C are patterns from Lilljuthatten including three samples with biotitic alterations, but no mineralization. D is patterns for samples collected away from Lilljuthatten.

Eleven of seventeen samples contain at least 0.25 weight per cent fluorine (Table 5). The uranium content of non mineralized granite varies from 4.74 to 49.11 ppm (Table 1) and averages 23.9 ppm. The thorium content for all of the analyzed granite varies from 19.13 to 101.8 ppm (Table 1) and averages 51.5 ppm. These values are markedly high by comparison to typical ranges for granitic rocks (U=3 to 5 ppm, Rogers and Adams 1969a, and Th=10 to 20 ppm, Rogers and Adams 1969b). The ranges for uranium and thorium in the Olden Granite area are similar to those calculated for a peraluminous granite from the Granite Mountains, Wyoming (Stuckless and Nkomo 1978). It has been shown that this granite was most likely derived from an evolved source (Stuckless and Miesch 1981). This granite differs from the Olden Granite in that it is strongly peraluminous.

A ternary plot of normative quartz, albite, and orthoclase (Fig. 11) shows that most of the data plot below the polybaric minimum of the haplogranite system (Tuttle and Bowen 1958; Luth and others 1964) and occupy the same region of the

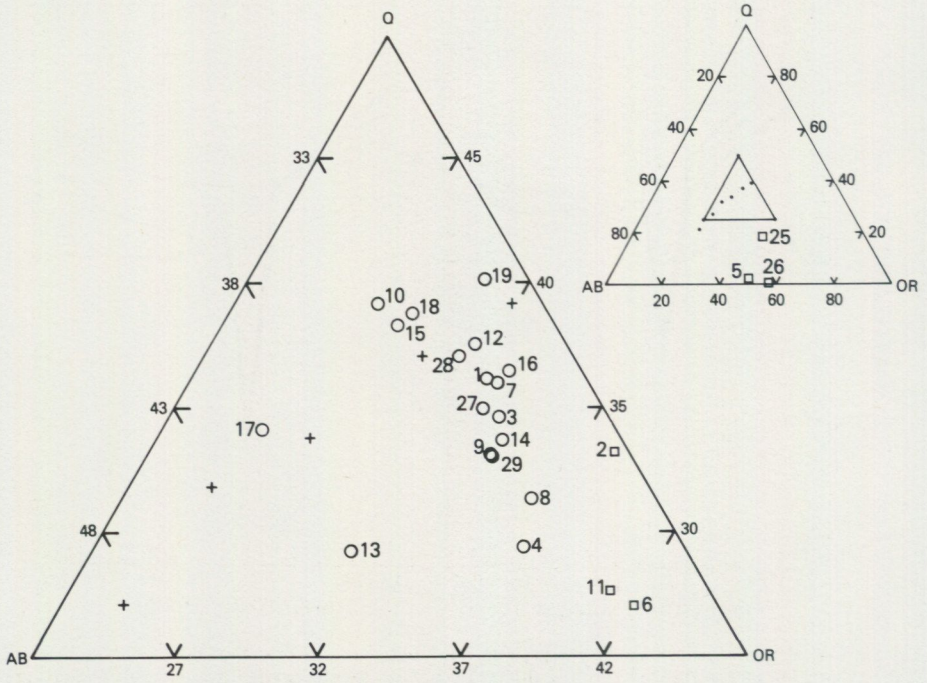

Fig. 11. Ternary diagram for normative quartz, albite, and orthoclase for samples from the Olden Granite, Sweden, with the polybaric minima from the water-saturated haplogranite system at 0.5, 1,2,3, and 5 kb shown by crosses (Tuttle and Bowen 1958; Luth and others 1964). Samples with biotitic alteration are indicated by squares. Apparently unaltered samples shown by circles. Numeric identification corresponds to symbol in Table 5. Three data points for altered samples that plot outside of the expanded portion of the diagram are shown on the insert.

diagram as has been found to be most common for peraluminous granites (Luth and others 1964). Most of the data fall along a fairly linear trend that intersects the ternary minimum trend between 0.5 and 1.0 kb water pressure. A similar trend for granitic liquids has been interpreted to be the result of derivation by partial melting under high pressure and water-undersaturated conditions followed by differentiation with decreasing pressure and increasing water activity (Stuckless and O'Neil 1973). A similar interpretation for the trend on Figure 11 does not seem reasonable because the differentiation indices do not change in any uniform manner along the trend. The sample with the lowest differentiation index is not on the trend, and the trend is approximately parallel to or overlapping with that formed by the samples with biotitic alteration. Furthermore, the trend is in part correlative with conclusions about open-system behaviour reached on the basis of isotopic data, as discussed below. In addition, normative feldspar data (Fig. 11) suggest that most of the granite crystallization occurred at a uniformly low partial pressure of water.

Six of the analyzed samples exhibit effects of biotitic alteration. Three of these samples are mineralized and three are not. There are also three samples that are mineralized, but are apparently unaffected by the biotitic alteration. These facts suggest that biotitic alteration and mineralization are two separate events.

The effects of biotitic alteration and mineralization on the chemistry of the granite can be seen in Figures 9, 10, 11, and 12. In general, the chemistry of the mineralized samples is not markedly distinct from that of the non-mineralized samples. In contrast, the biotitic alteration has profoundly changed the composition of the granites. This is most obvious for the contents of SiO_2, Al_2O_3, FeO, MgO, Na_2O, and K_2O (Table 5). Surprisingly, neither biotitic alteration nor mineralization produced an observable change or pattern in the whole rock $\delta^{18}O$ values (Table 10).

Biotitic alteration caused varying degrees of increase in the contents of FeO, MgO, Al_2O_3, K_2O, and K_2O/Na_2O ratio as reflected in the relative increase of normative orthoclase for five of six altered samples (Fig. 12), and an increase in the degree of alumina saturation for four samples (Fig. 9). Silica contents have been variably decreased (Table 5) with a concomitant decrease in normative and modal quartz (Fig. 11 and Table 8). Other elemental concentrations listed in Table 5 are apparently unaffected. Rare-earth contents for the unaltered samples are remarkably similar, especially those from the limited area of Lilljuthatten (Fig. 10), such that even small changes in rare-earth content should be observable. However, the rare-earth patterns for the samples with biotitic alteration are not discernibly different. A lack of response of rare-earth contents to other types of hydrothermal alteration has been noted in the granite from the Granite Mountains, Wyoming (Stuckless and Miesch 1981).

There is a suggestion that some of the unaltered and mineralized samples have incurred a small increase in the degree of alumina saturation (points 1 and 3, Fig.

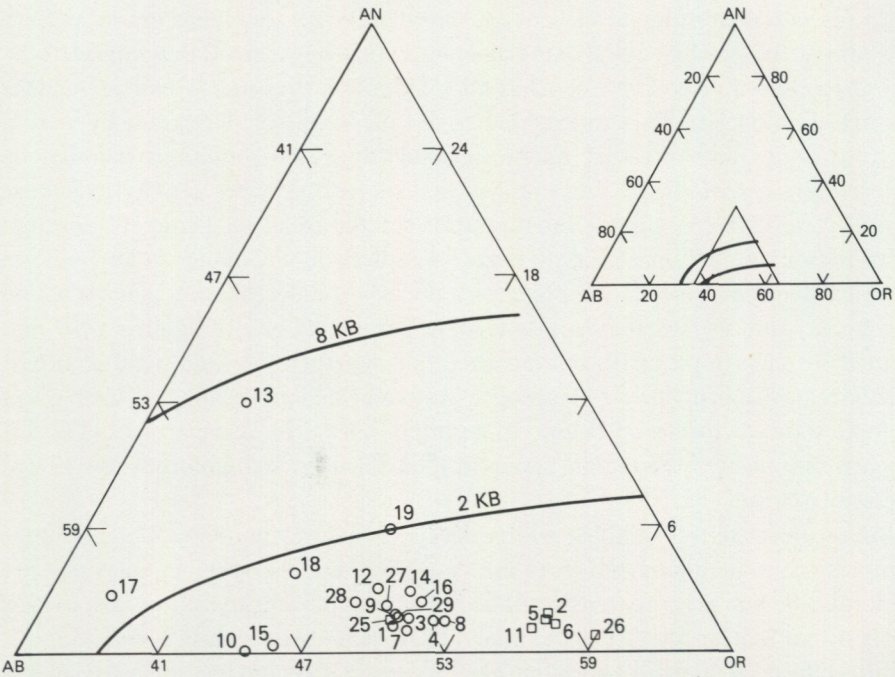

Fig. 12. Ternary diagram for normative anorthite, albite, and orthoclase for samples from the Olden Granite, Sweden, with univariant curves for water-saturated systems at 2 and 8 kb (from Whitney 1975). Samples with biotitic alteration shown by squares. Other samples shown by circles. Numeric identification corresponds to symbol in Table 5.

9). However, these and the other mineralized and unaltered samples are not distinguishable from the non-mineralized samples in the normative haplogranite and normative feldspar systems (Figs. 11 and 12). The two most strongly mineralized samples (both of which are also biotitic) exhibit a smaller europium anomaly than any of the other samples (Fig 10). The biotitic alteration has had a more pronounced chemical effect on other samples which do not show a decreased europium anomaly relative to unaltered samples. It therefore seems likely that the smaller europium anomaly for the two most strongly mineralized samples developed in response to mineralization. However, the rest of the rare-earth contents for even these samples is within the range observed for the unaffected samples.

AGE OF MINERALIZATION

All of the lead-lead data for the six mineralized whole-rock samples analyzed for this study and the lead-lead data for five unmineralized whole-rock samples from Lilljuthatten form a linear trend (Figs. 13 and 14). The data do not fit an isochron

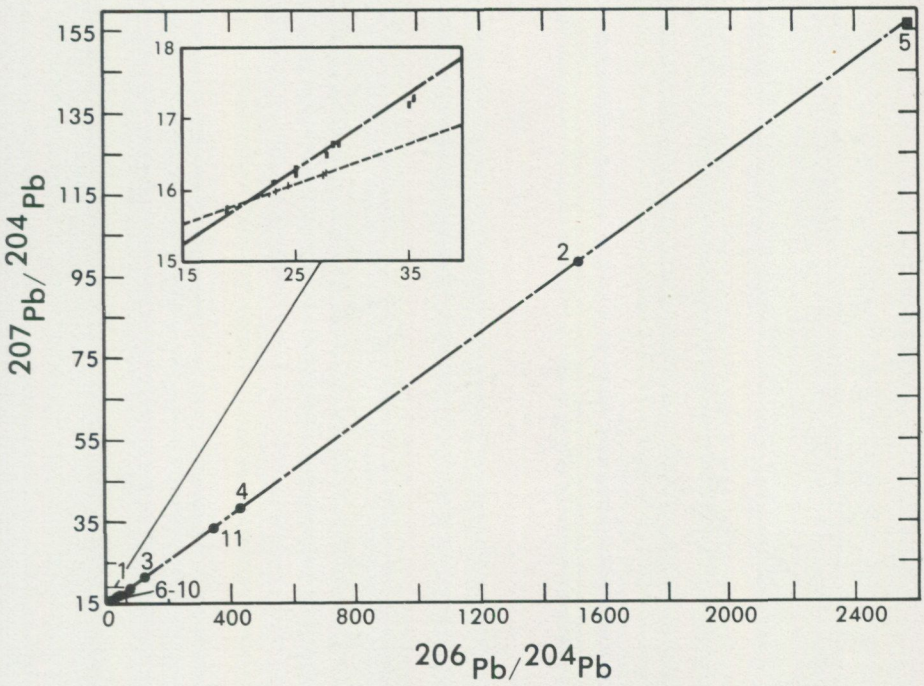

Fig. 13. Lead-lead diagram for six mineralized and five unmineralized samples from Lilljuthatten, Sweden. Regressed line yields an age of 420 ± 3 Ma. Numeric identifications correspond to plot I.D. (Table 1).

within the limits of analytical precision. However, significant variations in the initial lead compositions might reasonably be expected by virtue of a long history prior to mineralization.

A constant initial composition of lead for all samples at the time of mineralization would exist only for highly specialized circumstances such as a complete loss of radiogenic lead at the time of mineralization or equal U/Pb ratios in all samples from time of crystallization through time of mineralization. The former special case can be eliminated as a possibility because the common lead required at the time of crystallization would be unreasonable in view of the geologic history of the area, and as discussed below, a common lead can be determined which is consistent with the age of crystallization and markedly different from one that would fit the linear array formed by the mineralized samples. The second specialized case would be atypical relative to data published for other granites. Furthermore, samples that do not fit the mineralized Pb-Pb trend preserve evidence of variable inital U/Pb ratios.

The close fit to linearity for eleven samples in the lead-lead system suggest a

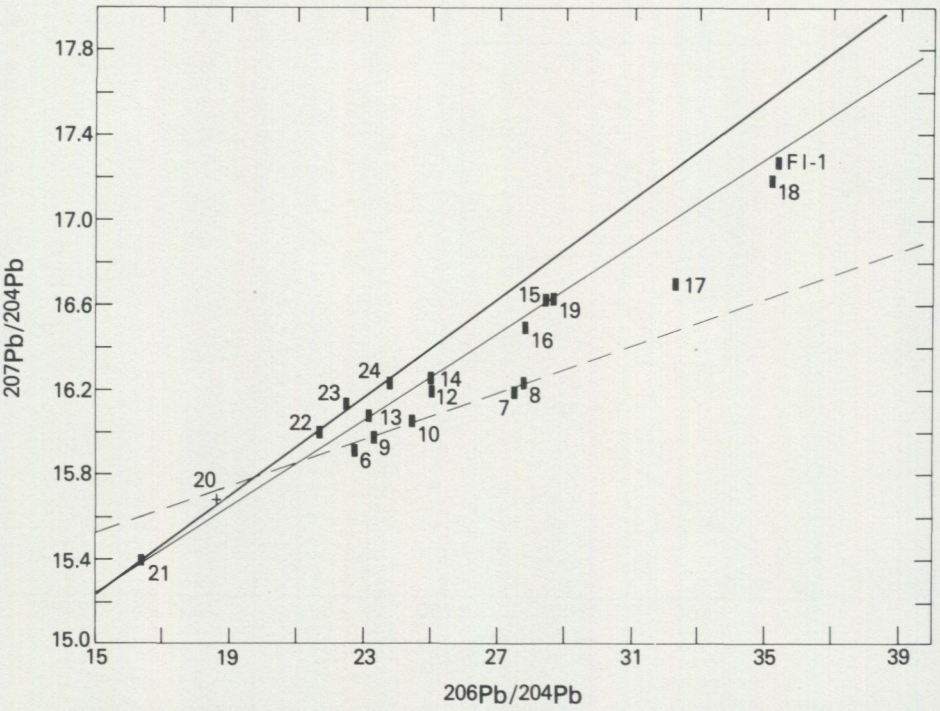

Fig. 14. Lead-lead diagram for whole-rock and mineral data with low radiogenic lead compositions from the Olden Window, Sweden. Symbol sizes correspond to $\pm 2\sigma$. Numeric identifications correspond to plot I.D. (Tables 1 through 3). The line with the shallowest slope is regressed through points 1 through 11 and corresponds to an age of 420 ± 3 Ma. The line with the intermediate slope is regressed through points 13, 14, 15, and 19 and yields an age of 1 667 ± 56 Ma. The steepest line is regressed through data for the four galena analyses (points 21 through 24) and one potassium feldspar corrected for accumulation of radiogenic lead from 420 Ma to the present (point 20 shown by cross). This line is a secondary isochron that corresponds to an age of 1 650 + 575/−885 Ma assuming that the isochron developed at 420 Ma ago. All ages quoted at the 95 per cent confidence level.

surprising degree of isotopic homogenization at the time of mineralization. If it is assumed that the distribution of initial lead compositions at the time of mineralizations is normal, then the linear array can be regressed and a corresponding age can be calculated (Ludwig 1979). This regression results in a slope of 0.05518 ± 0.00007 and an intercept of 14.696 ± 0.041 which corresponds to an age of 420 ± 3 Ma. No other dates for mineralization are available for comparison, but this age is in good agreement with a reset K-Ar age for biotite from the Olden Window (418 ± 3 Ma, Klingspor and Troëng 1980).

AGE OF THE GRANITE

None of the isotopic systems investigated in this study have completely retained the age of granite crystallization. However, several lines of evidence suggest that the granite is older than previously suspected and may be about 1 650 Ma old.

A concordia plot for four zircon fractions from one sample shows that all the analyses are strongly discordant (Fig. 15). The results do not fit a straight line within the limits of analytical precision, and the lower-intercept age (260 ± 10 Ma) does not correspond to any known geologic event. These observations can be explained by a three-stage isotopic history of (1) crystallization, (2) lead loss during the Caledonian, and (3) a second lead loss in response to Tertiary or Quaternary uplift and erosion. The upper-intercept age of 1 570 ± 20 Ma is interpreted as a minimum age.

The fluorite analysis from a sample Lill-1 is nearly concordant (Fig. 15). Addition of this analysis to the zircon regression does not significantly change

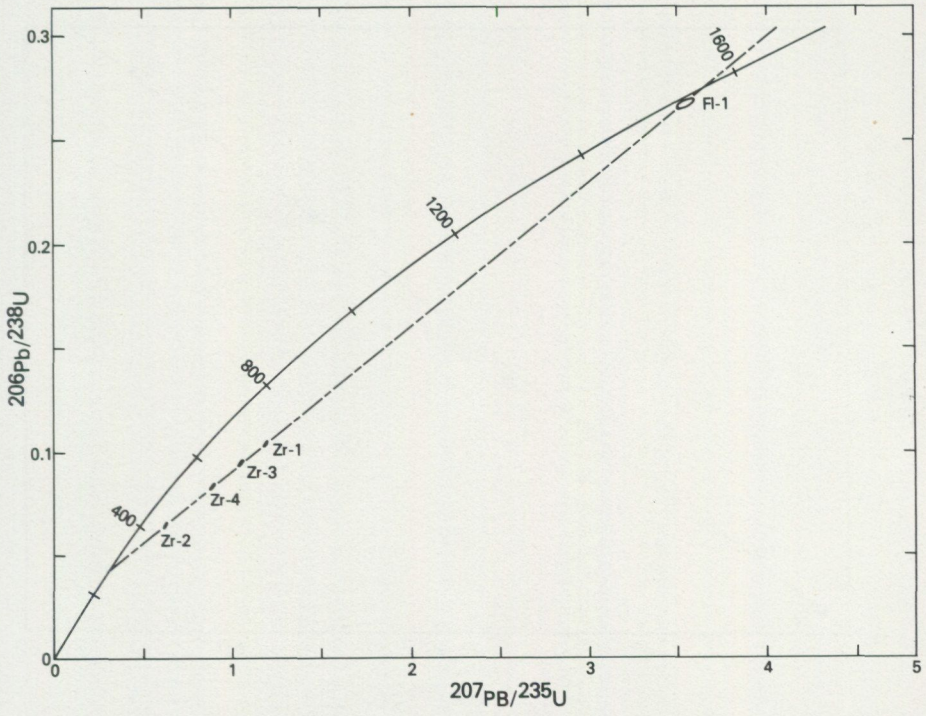

Fig. 15. Concordia diagram for four fractions of zircons (Table 2) from samples Lill-1. Symbol size corresponds to $\pm 2\sigma$. Intercept ages are 1 570 ±20 Ma, and 260 ± 10 Ma. Also shown, but not used in the regression of the line, is the data for fluorite for the same sample.

either the upper or lower intercept on concordia; although the upper intercept error is nearly halved. If it is assumed that the fluorite was effected by only the Caledonian event, the fluorite yields a crystallization age of 1 600 ± 65 Ma.

Whole-rock rubidium-strontium data do not yield an isochron (Fig. 16). Whole-rock and mineral data (Klingspor and Troëng 1980) document considerable redistribution of rubidium and/or radiogenic strontium during the Caledonian. Petrographic and chemical data show that many samples were affected by potassium metasomatism which probably occurred during the Caledonian. If it is assumed that rubidium was added with potassium, the effect on the strontium evolution plot (Fig. 16) would be to displace samples to higher values of $^{87}Rb/^{86}Sr$.

Four samples are co-linear on a strontium evolution plot with all but one of the remaining samples displaced to higher $^{87}Rb/^{86}Sr$ values. The four co-linear samples are physically separated from known areas of mineralization (Fig. 2) and therefore these may have been least effected by the Caledonian mineralization.

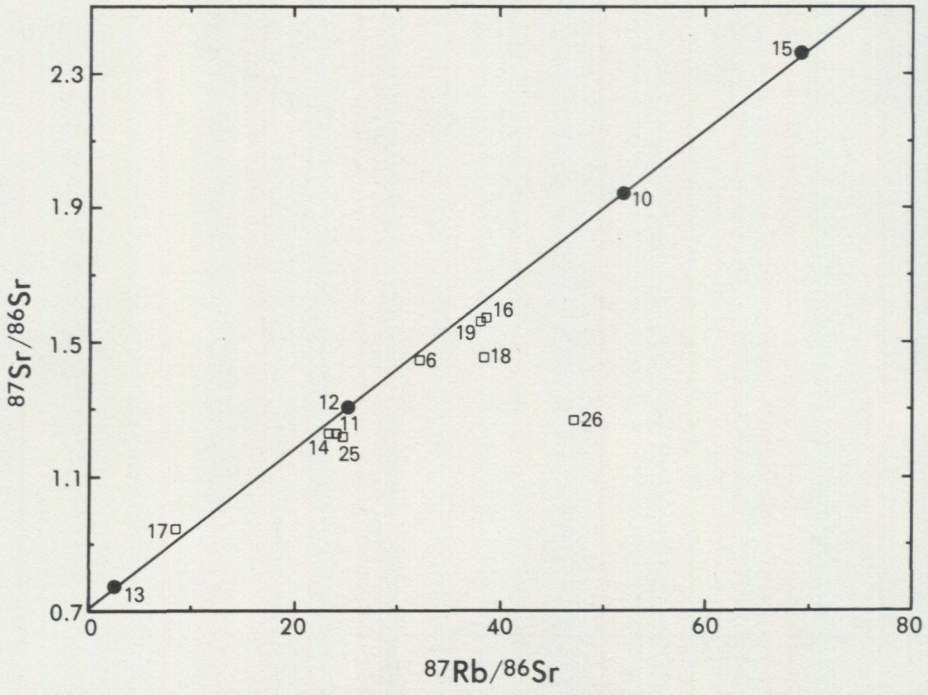

Fig. 16. Rubidium-strontium diagram for whole-rock data from the Olden Granite, Sweden. Numeric identification corresponds to plot I.D. (Table 4). The regressed line through points 10, 12, 13, and 15 yields an age of 1 640 ± 10 Ma at the 95 per cent confidence level.

Regression of the data for the presumed least disturbed samples yields a line within the limits of analytical error with a slope of 0.02357 ± 0.00014 and an intercept of 0.70980 ± 0.00060. The resulting age is 1 640 ± 10 Ma. This initial ratio is slightly high relative to those derived for initial lead ratios, but not anomalous relative to initial $^{87}Sr/^{86}Sr$ ratios for other granites of similar age in Sweden (Wilson and Sundin 1979).

Lead-lead data for samples that do not fit the mineralized-samples isochron are not co-linear (Fig. 14). However, if samples along a line with the smallest slope represent a near-complete resetting at the time of mineralization, samples along the line of steepest slope may represent the least amount of resetting. Samples between two such lines represent varying amounts of resetting between the two extreme cases.

Four samples (13, 14, 15, and 19) are co-linear within the limits of experimental error and plot along a line of steepest slope. If it is assumed that all open-system behavior would have affected all samples in the same direction, regression of these four samples yields a minimum age of crystallization. This assumption is important because special circumstances can be invoked that would result in a linear array for which the corresponding age would be erroneously old. Regression of the four samples yields a slope of 0.10236 ± 0.00307 and an intercept of 13.704 ± 0.081 which corresponds to an age of 1 667 ± 56 Ma. This is in good agreement with that estimated from the rubidium-strontium data.

The lead-lead data for feldspar and galena can be used to obtain an independent estimate of the age of crystallization of the granite. Galena mineralizations are found in Caledonian structures. If it is assumed that the galenas formed at the time of uranium mineralization and that the granite was the source of the lead as discussed below, then the galena analyses should form a linear array. Furthermore, this array should be co-linear with lead from a granitic feldspar that was affected by the Caledonian event because all these leads would represent mixtures of the common lead for the granite and lead that accumulated in the granite by the decay of uranium from the time of crystallization to the time of mineralization.

Data for four galenas (Table 3) and one potassium feldspar (corrected for the growth of radiogenic lead from the time of mineralization to the present, Table 1) are co-linear on Figure 14, but not within the limits of analytical error. Thus the galenas may have a small component of lead from sources other than the granite such as the closely associated metavolcanics. Regression of the galena-feldspar linear array with the assumption that residual errors are normally distributed, results in a line with a slope of 0.11545 ± 0.40963 and an intercept of 13.506 ± 0.845 which corresponds to an age of 1 650 ± 575/-885 Ma (assuming that the secondary isochron formed at 420 Ma ago). Although the errors are large, the secondary isochron age is in agreement with those obtained by two independent methods and assumptions.

INTERPRETATION OF URANIUM AND LEAD MOBILITY

A unique interpretation of uranium and lead mobility is not possible with the available data because neither element has remained immobile, and the host granite has a three-stage isotopic history. Modelling the history of uranium and lead is further complicated by the imprecisely known ages of crystallization and late-stage remobilization of uranium. Nonetheless, a probable model can be developed that places limits on the amount and timing of mobility for both elements.

The ages used in modelling the history of uranium and lead are T_o the time of crystallization (T_o = 1 650 Ma), the age of first system disturbance (T_m = 420 Ma), and the age of second system disturbance (T_p = 0 Ma). The last age probably represents the introduction of groundwater into the system. No quantitative control exists for this age, but the regional geologic history and the observed disequilibrium within the ^{238}U decay chain (Table 7) suggest that something within the last few million years is reasonable, and the use of zero simplifies calculations.

There is ample evidence that lead was mobilized at 420 Ma. The isotopic composition of the potassium feldspar in Lill-1 (#20) was adjusted at that time; large amounts of galena formed, and most of the whole-rock samples from Lilljuthatten readjusted to a near-constant lead composition. Most of the whole-rock readjustment of lead composition must have occurred by the loss of radiogenic lead. Projection of each whole-rock data point back to the secondary isochron (along a line parallel to that with least slope on Figure 14) shows each of the samples that plots on the mineralized rock isochron contained a less radiogenic lead at 420 Ma than any of the other samples. Mineralized samples project to $^{206}Pb/^{204}Pb$ compositions of 19.512 to 20.691 whereas the remainig samples project to values of 21.474 to 28.703. It seems too fortuitous to attribute these differences to differences in the U/Pb ratios from the time of crystallization through to the time of mineralization.

The thorium-lead system provides strong evidence for lead loss that is predominated by a radiogenic component. A plot of the thorium-lead data (Fig. 17) does not yield an isochronal relationship among any samples, but a few general features can be observed. The samples that define the mineralized Pb-Pb isochron come closest to approximating a slope that corresponds to an age of 420 Ma. Only one sample from this group projects to a higher $^{208}Pb/^{204}Pb$ ratio at 420 Ma than the least radiogenic lead of the remaining samples. All but one of the samples plot to the right of a reference isochron with a slope corresponding to 1 650 Ma and a lower intercept similar to that predicted by a Stacey and Kramers (1975) lead evolution model.

The foregoing observations can be explained by either thorium gain or radiogenic lead loss. However, if thorium gain is chosen as the explanation, a special set of

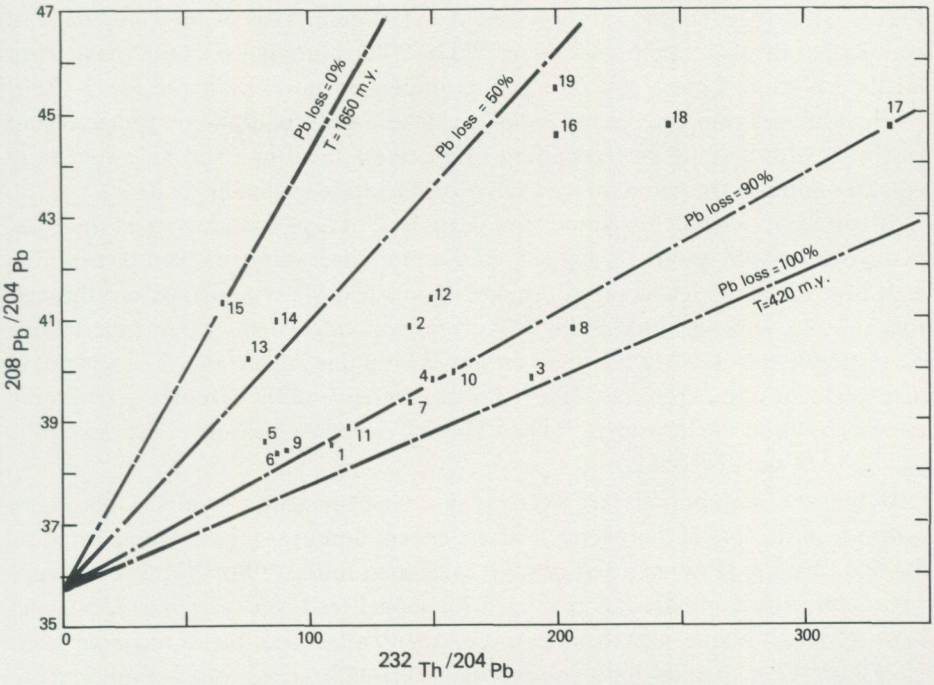

Fig. 17. Thorium-lead diagram for whole-rock data from the Olden Granite, Sweden. Numeric identification corresponds to plot I.D. (Table 1). Symbol size corresponds to $\pm 2\sigma$. Also shown are lines corresponding to 0, 50, 90, and 100 per cent radiogenic lead loss at 420 Ma assuming a crystallization of 1 650 Ma and no lead loss for data point 15.

conditions is required. The samples that now form the mineralized isochron (in the Pb-Pb system) must have had the lowest Th/Pb ratios from 1 650 to 420 Ma ago. For these samples, the amount of thorium gain must have been roughly proportional to the Th/Pb ratio. This mechanism did not operate for all samples, otherwise all would approximate a line with a slope corresponding to an age of 420 Ma. Furthermore, the thorium gain must be completely independent of the uranium gain as there is no correlation between uranium and thorium contents for the samples that define the mineralized isochron. The fact that the two elements should not correlate is suggested by the low thorium content of the analyzed pitchblendes (Table 9). Finally, thorium has a close geochemical coherence to the rare-earth elements and the patterns for these elements in both mineralized and non-mineralized samples suggest immobility. Thus all of our data agree with the conclusion that thorium is not particularly mobile in most geologic environments (Manton 1973; Stuckless and Nkomo 1978; Zielinski and others 1981).

The preferential loss of radiogenic lead provides a more reasonable explanation for the pattern observed on Figure 17. Displacement of points by lead loss on

Figure 17 can be envisioned as a two vector system. Loss of the common lead component displaces points to higher $^{232}Th/^{204}Pb$ values but does not move them off the isochron. Loss of the radiogenic component moves points to lower $^{208}Pb/^{204}Pb$ values. A complete loss of radiogenic lead would result in points defining an isochron with a slope corresponding to the age of lead loss and an initial ratio corresponding to the common lead value for the time of crystallization.

In order to define the amount of lead loss, it was assumed that the least disturbed sample (point 15, Fig. 17) in the thorium-lead system had incurred no lead loss. A line with a slope corresponding to 1 650 Ma was then passed through this sample, and an initial $^{208}Pb/^{204}Pb$ ratio was calculated. A line with a slope corresponding to 420 Ma was then projected from this initial ratio. The amount of displacement parallel to the $^{208}Pb/^{204}Pb$ axis (relative to the distance between the two isochrons at the measured $^{232}Th/^{204}Pb$ ratio) is then a measure of the radiogenic loss 420 Ma ago (Table 11).

If the age assumptions are correct, this measurement provides a minimum estimate of the loss of thorogenic lead in per cent because of the assumed zero loss for one sample. However, because the calculated initial $^{208}Pb/^{204}Pb$ ratio is approximately the same as that predicted for model lead (35.747 *versus* 35.50) and because much higher initial ratios (necessary to allow lead loss for sample point 15, Figure 17 or to allow for a younger age of crystallization) would result in more than 100 per cent lead loss for sample point 3, the calculated lead losses must be approximately correct. Alternatively larger lead losses could be calculated by assuming an older age of crystallization.

Once the amount of lead mobility has been established, it is possible to interpret the amount of uranium mobility by assuming that movement of thorogenic and uranogenic losses were equal. This assumption may underestimate the uranogenic lead loss because commonly a larger proportion of the uranium, relative to thorium, is located in labile sites (Stuckless and Nkomo 1980). Hence, a larger proportion of the uranogenic lead is in contact with interstitial fluids.

The amount of uranium mobility, relative to lead can be obtained from the concordia system (Fig. 18). This treatment of the data uses only the radiogenic portion of the lead and thus the composition of the common lead must be obtained. This lead composition must lie on both the secondary isochron defined by the galenas and the primary isochron defined by the least disturbed samples. The intersection of these two isochrons is $^{206}Pb/^{204}Pb = 15.113$ and $^{207}Pb/^{204}Pb = 15.251$.

The whole-rock data scatter about a line that intersect concordia at 1 550 ± 40 Ma and 400 ± 70 Ma (Fig. 18). If the rocks had been affected by only the crystallization and mineralization events, the data would plot along a line that intersects concordia at 1 650 and 400 Ma. However, the insert on Figure 18 shows that the samples which were most completely reset during the mineralization

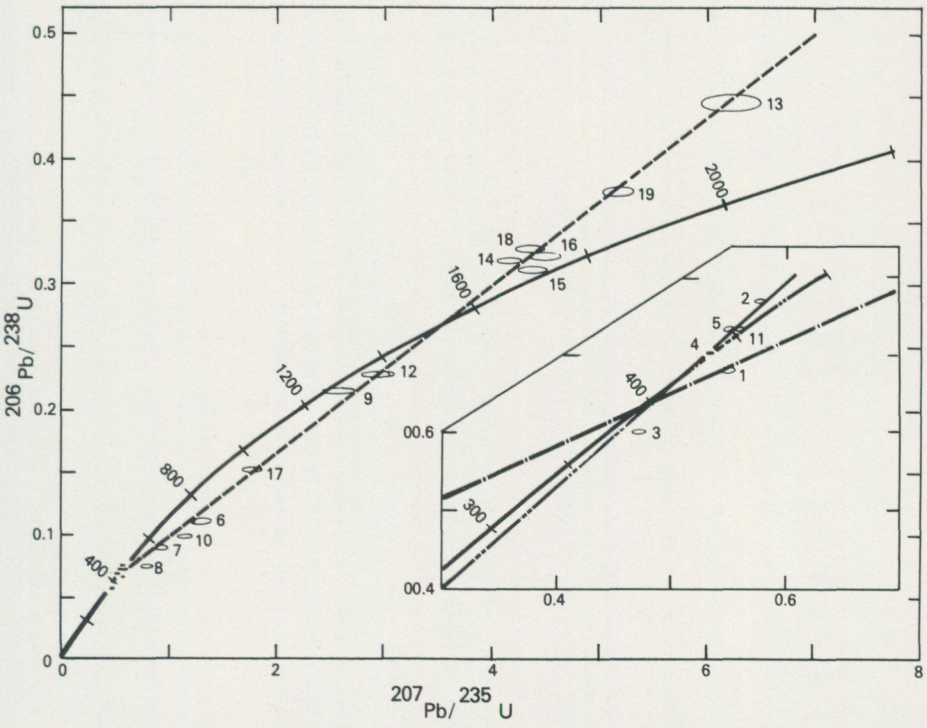

Fig. 18. Concordia diagram for whole-rock data from the Olden Granite, Sweden. Numeric identification corresponds to plot I.D. (Table 1). Symbol size corresponds to $\pm 2\sigma$. Insert shows detail of lower intercept with a reference line that intersects concordia at 0 and 420 Ma. Regressed line yields intercepts of 1 650 ± 40 and 400 ± 70 Ma.

event scatter along a second chord from zero through 420 Ma. Four of these six samples have lost 3 to 13 per cent uranium relative to lead during the last few million years. This loss probably corresponds to the observed alteration of some pitchblende grains (Fig. 8).

The amount of recent uranium mobility can be calculated by assuming lead immobility from 420 Ma to the present. Each data point would then lie on the cord that connects 420 and 1 650 Ma. The intersection of that chord and one joining each sample with the origin yields the plot of the data prior to recent uranium mobilization, and the distance of a plotted point from that intersection is proportional to the amount of uranium gain or loss (Table 11).

The amount of uranium gain or loss at 420 Ma is obtained by subtracting the amount of radiogenic lead that would have accumulated by the decay of uranium and thorium during the last 420 Ma from the total observed radiogenic lead. The uranium concentration used in this calculation is the value as adjusted for recent gain or loss of uranium. The thorium value used is the measured concentration.

Table 11. Model changes for uranium and lead concentrations in per cent at 420 Ma ago and for recent changes in uranium concentration.

Sample number	Pb	U 1st change	U recent change	Plot I.D.
77660	-93.0	302	4.8	1
77662	-78.6	7360	-13.1	2
77666	-99.2	-15.3	15.8	3
77735	-90.6	54800	-3.4	4
77738	-72.8	8220	-9.2	5
77968	-86.8	-58.2	23.9	6
77972	-92.7	-49.1	10.4	7
77979	-94.6	-67.5	39.0	8
77981	-85.6	-56.4	-34.3	9
79061	-91.5	-71.0	35.2	10
79911	-91.0	7050	-7.8	11
76032	-73.8	-49.8	-19.2	12
76285	-40.4	-40.3	-34.6	13
77988	-39.3	-33.3	-15.8	14
79062	0	-3.8	-3.4	15
79070	-64.0	-44.7	-34.8	16
79903	-91.0	-65.0	-18.1	17
79914	-75.5	-57.2	-38.6	18
Lill-1	-56.8	-52.3	-27.7	19

The thorogenic lead (remaining after subtraction of the post-mineralization lead) is then compared to the equilibrium amount of ^{208}Pb required by the measured thorium for the time period 1 650 to 420 Ma ago. This determines the percentage of radiogenic lead loss at 420 Ma, and the uranogenic lead is increased accordingly. The pre- and post-mineralization lead contents are recombined, divided by the adjusted (for recent mobility) uranium contents, and plotted on Figure 19. The distance of displacement of any point from the point on concordia that represents the age of crystallization is a measure of uranium mobility at 420 Ma (Table 11).

The model shown on Figure 19 suggests that most of the granite lost between 30 and 70 per cent of its uranium at the time when samples from the ore deposit gained more than 50 000 per cent uranium. Because of the number of assumptions needed to model the data, the conclusions for any one sample may not be correct in detail, but the overall pattern suggests most of the granite contained 30 to 80 ppm uranium up until the time of the Caledonian orogeny and that mobilization of

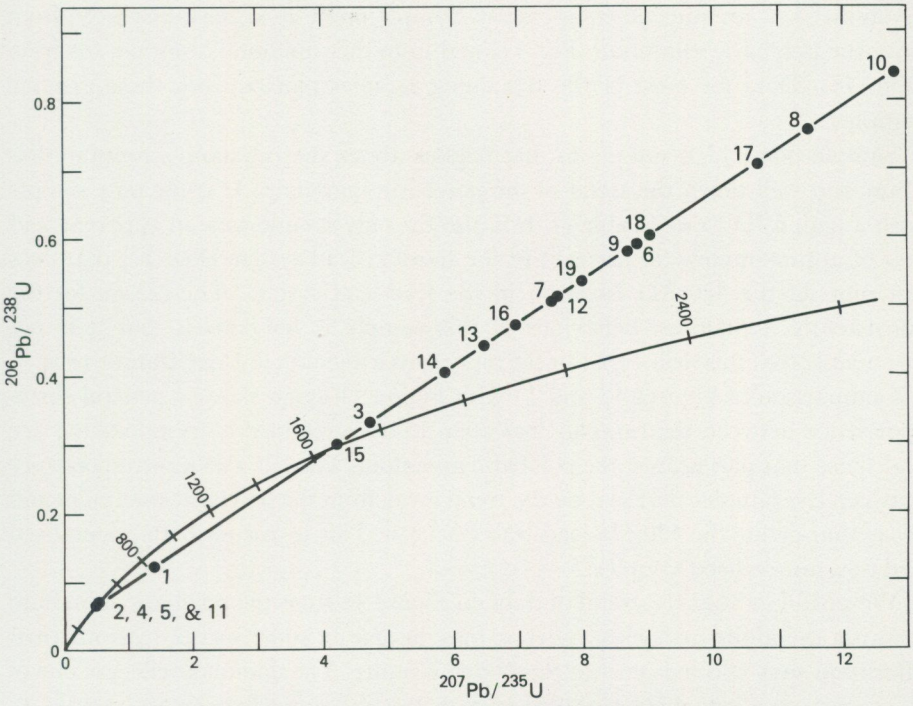

Fig. 19. Concordia diagram for model whole-rock data from the Olden Granite, Sweden. Numeric identification corresponds to plot I.D. in Tables 1 and 9. Intercepts on concordia are 1 650 and 420 Ma.

uranium resulted in a lowering of the average uranium content in most places and deposition of ore in others. Similar high uranium contents have been calculated for granites with a less complex history (Rosholt and others 1973; Stuckless and Nkomo 1978), and have been measured for granites recovered from a deep drill-hole (Rosholt and Huestis 1981).

AGE OF BIOTITIC ALTERATION

The mobilities postulated for uranium, lead and rubidium may be reflected in the major element data. Comparison of Figures 11 and 16 shows that data for three of the four samples yield the isochronal age of 1 650 Ma. All plot near the ternary polybaric minimum. The fourth sample (point #13) is widely separated from all the rest of the samples in both the granite and feldspar systems and has the lowest differentiation index. This sample may not represent an equilibrium product

crystallized at an eutectic composition. Sample point 26 is most displaced from both the polybaric minimum (Fig. 11) and from the rubidium-strontium isochron (Fig. 16). Data for most of the remaining samples plot between these extreme samples.

Sample point 17 is unique in that it plots above the rubidium-strontium diagram and well down the trend of the polybaric minimum. It is the only sample with a high $\delta^{18}O$ value (Table 7). It is also the only sample with an apparent lead loss of approximately 90 per cent in the thorium-lead system (Fig. 17) that does not plot on the 420 Ma isochron in the lead-lead system. The reason for the consistently anomalous behaviour of this sample is not known, but it is not impossible that this drill-core sample represents a xenolith of older granitic rock.

Comparison of Figures 13 and 14 with Figure 11 again shows a general correspondence between the samples that seem to have retained a crystallization age and those that plot nearest the polybaric minimum. There is also a correspondence between the samples that plot on the trend away from the polybaric minimum and those that define the 420 Ma lead-lead isochron. This is true for both mineralized and non-mineralized samples.

We postulate that the trend of data on Figure 11 from the polybaric minimum towards the albite-orthoclase sideline may be due to some sort of hydrothermal alteration that affected most of the Olden Granite. The dominant effect is one of silica loss or alkali metasomatism with potassium gained in excess relative to sodium. There may also have been a destruction of magnetic minerals which would account for the pronounced aeromagnetic low in the northeastern part of the Olden Window. The timing of this event is unknown, but because several non-mineralized samples, (including one sample with biotitic alteration) that plot along this trend also plot along the 420 Ma lead-lead isochron, it seems likely that biotitic alteration and mineralization were nearly contemporaneous. Alternatively the biotitic alteration may have occurred some time prior to mineralization and pre-conditioned the altered rocks such that they were more susceptible to open-system behaviour at the time of mineralization. Although both possibilities explain the rubidium-strontium data equally well, the former is most consistent with the lead data. Furthermore, the biotitic alteration petrographically post-dates the main metamorphic stage of mineral petrogenesis.

MODEL FOR ORE FORMATION

The general model for ore formation at Lilljuthatten is one of (1) generation of a favourable granite that acted as both source of and host to the ore, (2) preparation of the host by fracturing, (3) mobilization of uranium in response to the Caledonian event, and (4) preservation of the deposit until recent, minor modifications. This model suggests that deposits similar to that at Lilljuthatten may reasonably

be discovered elsewhere in the Caledonides because granites which are generally similar to the Olden Granite are also fairly common.

The first step in the formation of the ore deposit at Lilljuthatten was the generation of a highly evolved granite. The fact that the granite was highly evolved is demonstrated by high contents of incompatible elements such as uranium, thorium, rubidium, and the rare-earth elements. Other features include the uniformly high differentiation index and large europium anomaly as well as high Rb/Sr and low K/Rb ratios (although it is possible that these ratios are in part secondary features). The protolith did not necessarily have a large sedimentary, or at least a large pelitic, component because the granite is not strongly peraluminous and $\delta^{18}O$ values are not particularly high. A granite with the features of the Olden Granite is most likely the product of a low degree of partial melting of crustal rocks.

Although it is likely that the protolith was enriched in rubidium, thorium, and uranium relative to strontium and lead, initial isotopic ratios for strontium and lead are not high. This probably indicates a short crustal history for the protolith rather than a diagnostic feature. A short crustal history is in keeping with the oldest known rocks in this part of Sweden (Wilson and Sundin 1979) which are only a few hundred million years older than the age obtained for the Olden Granite in this study.

A critical feature in the formation of the granite is that it was both highly enriched in uranium and that much of the uranium was located in labile sites such that introduction of fluids could readily mobilize uranium. The data and conclusions of this study indicate that the original distribution of uranium has been largely destroyed, but through mineralogical investigations of the Olden Granite (Smellie 1982), reasonable inferences as to the labile uranium sites can be made.

The Olden Granite is mineralogically similar to other high uranium granites that contain small amounts of uraninite (Basham and others 1979), and it contains both epidote and biotite which have been identified as sites for labile uranium in other studies (Stuckless and Nkomo 1980). In addition, the Olden Granite contains abundant iron and iron-titanium oxides with which uranium is associated (Smellie 1982), suggesting, in addition to the above features, that the Olden Granite could readily lose uranium. The only obvious characteristics that indicate the granite was initially high in uranium are the high uranium content of zircon (Table 2) which has been noted for granites associated with other uranium deposits (Silver 1976), and the generally high thorium content (Table 1) which has also been noted for high-uranium granites (Stuckless and Nkomo 1978; Rosholt and Huestis 1981).

The most important feature in host rock preparation seems to be intense fracturing although biotite in-filling may have been of local importance. The timing of these events cannot be determined exactly, but the fracturing is extensive

and generally parallel to regional Caledonian structures, and in the western part of the window, fracturing continues into the overthrust nappes. The biotite in-filling must post-date fracturing, and at least one biotized and non-mineralized sample yields results consistent with a Caledonian age. This is reasonable because emplacement of the nappes on the basement caused a rise in temperature which could initiate a circulation of hydrothermal solutions. These solutions might reasonably cause recrystallization and mobilization of biotite into fracture zones and other sites of low pressure. Thus, it seems likely that both fracturing and biotite in-filling occurred in response to the Caledonian orogeny.

The mobilization and precipitation of uranium are at present poorly understood. We have no quantitative data on fluid compositions or on limits for intensive variables such as pressure and temperature. The abundance of vein fluorite in Caledonian structures and the regional occurrence of carbonate rock and minor calcite veining in the nappes suggest that both fluorine and CO_2-rich fluids were possible. In either case, it is likely that some uranium precipitation occurred in open fractures in response to a pressure change with consequent loss of volatiles as proposed for the Hercynian deposits of France (Leroy 1978). Alternatively, the localization of uranium near the biotite in-fillings and dolerite dykes may suggest a redox reaction for which high iron content was important in the precipitation of uranium. This hypothesis is supported by chemical data which show a general increase in the ferric/ferrous ratio, for the sequence normal granite to biotitically altered granite to mineralized granite.

As mentioned earlier, there is an obvious spatial association between the uranium mineralization and the dolerite dykes. It therefore seems likely that the dykes had some role in the control in ore deposition. In addition to a possible redox-boundary hypothesized above (Troëng 1982), the pair of dykes may have acted to channel hydrothermal solutions or they may have responded to Caledonian stress in a manner different from that of the granite such that fracturing of the granite was most intense near the intersection of the dykes.

Limited data suggest that neither high temperature nor steep temperature gradients were critical factors in formation of the deposit and that frictional heat in response to thrusting was sufficient to drive necessary reactions. The effects of thrusting and metamorphism were most intense to the west (Andreasson and Lagerblad 1980) and yet uranium deposits were formed throughout the window (Troëng and Wilson 1979). It therefore does not seem that the location of the Lilljuthatten deposit in the parautochthonous block at the east side of the window is controlled by temperature gradient. Low temperature for ore deposition is suggested by the low thorium content of pitchblende (Table 9); however, it is possible that this feature is due to immobility of thorium in the source rock and hence a lack of thorium in the ore fluid rather than conditions during precipitation.

The final stage for the deposit at Lilljuthatten must have been one of deep

enough burial to prevent destruction of the ore by ground-water leaching. Pitchblende in some samples have been oxidized and altered (Fig. 8). Disequilibrium within the uranium decay chain (Table 7) and the distribution of data points for the mineralized samples on Figure 18 indicate recent mobilization and loss of uranium. These features are most likely the result of leaching by oxidizing ground water. If the deposit had not been sequestered from such waters for most of its history, it would have been destroyed.

SUMMARY AND CONCLUSIONS

High contents of incompatible trace elements (Tables 1, 4 and 6), large europium anomalies (Fig. 10) and high differentiation indices (Table 5) for almost all of the analyzed samples show that the Olden Granite was derived from an evolved crustal source, probably by a low degree of partial melting. Generally low $\delta^{18}O$ values (Table 10) and a weakly peraluminous character, (Table 5, Fig. 9) indicate that pelitic materials were not of major importance in the protolith. Moderately low initial $^{87}Sr/^{86}Sr$, $^{206}Pb/^{204}Pb$, and $^{208}Pb/^{204}Pb$ ratios (Figs. 14, 16, and 17) are interpreted to be the result of a relatively short crustal history for the protolith.

None of the isotopic systems examined in this study have completely retained the intrusive age of the Olden Granite. The isotopic systems of most samples have been strongly to completely reset by the Caledonian orogeny. A few samples yield whole-rock Rb–Sr (Fig. 16) and Pb–Pb (Fig. 14) isochrons of approximately 1 650 Ma. Four galenas and one potassium feldspar analysis also yield an age of 1 650 Ma (Fig. 14), however, four fractions of zircon appear to yield a three stage isotopic history for which a minimum intrusive age of 1 570 ± 65 Ma (Fig. 15). The available data indicate that 1 650 Ma is a reasonable approximation for the age of intrusion.

The age of mineralization can be determined with a much higher degree of confidence. Six mineralized and four non-mineralized samples of the Olden Granite yield a lead-lead, whole-rock isochron of 420 ± 3 Ma (Figs. 13 and 14). This age corresponds with the end of the Caledonian orogeny as dated by K–Ar for biotite (418 ± 3 Ma, Klingspor and Troëng 1980). Mineralization was apparently preceded by both metamorphic recrystallization and at least one phase of hydrothermal alteration (Troëng 1982). Limited data suggest that these events pre-dated mineralization by time spans that are too short to detect isotopically.

At least part of the hydrothermal activity was pervasive and ubiquitous. Joint filling and veining with quartz, fluorite, calcite, and galena are noted over a wide area of the Olden Window. Alkali addition or silica loss (Fig. 11) and uranium and lead loss (Table 11) are common to most samples of the Olden Granite. More intense or different hydrothermal alteration is only known to be an important feature at Lilljuthatten. At this locality, extensive fracture and joint systems are biotized with and without uranium mineralization (Figs. 4, 5, and 7). Chemical

data, particularly in the Q–Ab–Or system suggest that this alteration may be a more extreme example of that observed in the rest of the granite (Fig. 11).

A final event noted in the isotopic and petrographic data is a redistribution of uranium that apparently occurred in response to the recent exposure of the granite to near surface conditions. Pitchblende is chemically and visibly altered (Fig. 8, Table 9) and many whole-rock samples have developed a pronounced disequilibrium within the ^{238}U-decay chain (Table 7). These observations show that the granite must have been sequestered from near-surface effects from Caledonian time though to the last few million years, or else the deposit would have been destroyed.

Uranium deposits, like the one at Lilljuthatten, might reasonably be expected elsewhere. Although the initial uranium content calculated for the Olden Granite is anomalously high (30–80 ppm), similar granites are known (Stuckless and Nkomo 1978; Rosholt and Huestis 1981). These granites, like the Olden Granite, are peraluminous. Overthrusting, which apparently prepared the granite structurally and provided heat for hydrothermal solutions, is also geologically common in the Swedish Caledonides. The transport and deposition mechanisms for uranium at Lilljuthatten require more study, but these may vary from locality to locality. Certainly, areas near dolerite dykes that cut favourable granites have high potential in other windows of the Caledonides. Several studies have suggested that uranium, especially in uraniferous granites, is readily mobilized (Manton 1973; Rosholt and others 1973; Oversby 1975; Stuckless and Nkomo 1978; Nkomo and others 1978, 1979; Stuckless and others 1981). It also seems that uranium, once mobilized, is readily precipitated by changes in temperature, pressure, or oxidation potential. It therefore is reasonable that the combination of source material, driving force, and appropriate depositional environment will be found elsewhere. Unfortunately, deposits similar to that at Lilljuthatten may also be volumetrically small and difficult to locate.

ACKNOWLEDGEMENTS

This study has benefitted greatly from the technical assistance of several persons. G. T. Cebula and J. W. Groen prepared samples and mineral separations. H. T. Millard, D. M. McKown, and R. J. Knight performed delayed neutron and instrumental neutron activation analyses. C. M. Bunker and C. A. Bush provided gamma-ray spectrometer analyses. B. A. Keaten performed radiochemical separation anlyses for rare-earth analyses of mineralized samples. J. W. Baker, J. S. Wahlberg, and A. J Bartel made the X-ray fluorescence analyses at the U.S. Geological Survey. Assistance in microprobe analyses was provided by B. Beddoe-Stephens of Institute of Geologic Services, London. The analyst from the Geological Survey of Sweden was G. Svedenback.

J. A. T. Smellie and M. R. Wilson critically read the manuscript at various stages during its development.

The Geological Survey of Sweden acknowledges the financial support obtained from the Swedish Nucleor Fuel Supply (SKSF).

REFERENCES

ANDREASSON, P. G., and LAGERBLAD, B., 1980: Occurrence and significance of inverted metamorphic gradients in the western Scandinavian Caledonides. — J. Geol. Soc. London 137: 219–230.

ASKLUND, B., 1938: Hauptzüge der Tektonik und Stratigraphie der mittleren Kaledoniden in Schweden. — Sver. geol. unders. C 417: 1–99.

— 1960: Studies in the thrust region of the southern part of the Swedish mountain chain. — Intern. Geol. Cong., Norden 1960, Guide to excursions A24 and C19: 1–60.

BARKER, F., MILLARD, H. T., Jr., HEDGE, C. E., and O'NEIL, J. R., 1976: Pikes Peak Batholith: Geochemistry of some minor elements and isotopes, and implications for magma genesis. — *In* R. C. Epis and R. J. Weimer, eds.: Prof. Contr. of Colorado School of Mines 8: 44–56.

BARNES, I. L., MURPHY, T. J., GRAMLICH, J. W., and SHIELDS, W. R., 1973: Lead separation by anodic deposition and isotope ratio mass spectrometry of microgram and smaller samples. — Anal. Chem. 45: 1881–1884.

BASHAM, I. R., VAIRINHO, M. M. B., and BOWLES, J. F. W., 1982: Uranium-bearing accessory minerals in the San Pedro do Sul granite, Portugal. — *In:* Vein-type and Similar Uranium Deposits in Rocks Younger than Proterozoic. — Proc. Tech. Comm. Meeting, Lisbon, IAEA, Vienna, 279—298.

BUMA, G., FREY, F. A., and WONES, D. R., 1971: New England granites: trace element evidence regarding their origin and differentiation. — Contr. Mineral. Petrol. 31: 300–320.

BUNKER, C. M., and BUSH, C. A., 1966: Uranium, thorium, and radium analyses by gamma-ray spectrometry (0.184–0.352 million electron volts). — *In* Geol. Survey Research 1966: U.S. Geol. Survey Prof. Paper 550-B: B176–B181.

BUNKER, C. M., and BUSH, C. A., 1967: A comparison of potassium analyses by gamma-ray spectrometry and other techniques. — *In* Geol. Survey Research 1967: U.S. Geol. Survey Prof. Paper 575-B: B164–B169.

EVENSEN, N. M., HAMILTON, P. J., and O'NIONS, R. K., 1978: Rare-earth abundances in chondritic meteorites. — Geochim. Cosmochim. Acta. 42: 1199–1212.

FRÖDIN, G., 1916: Einige Beobachtungen über den Oldengranit und die subkambrische Denudationsflache innerhalb der Kaledonischen Faltenzone in Jämtland. — Bull. Geol. Instit. Uppsala XIII: 233–386.

GEE, D. G., 1975: A geotraverse through the Scandinavin Caledonides — Östersund to Trondheim. — Sver. geol. unders. C717: 1–66.

— and ZACHRISSON, E., 1979: The Caledonides in Sweden. — Sver. geol. unders. C 769, 48 pp.

GORBATSCHEV, R., SOLYOM, Z., and JOHANSSON, I., 1979: The Central Scandinavian Dolerite Group in Jämtland, Central Sweden. — Geol. För. Stockh. Förh. 101: 177–190.

GORDON, G. E., RANDLE, K., GOLES, G., CORLISS, J., BEESON, M., and OXLEY, S., 1968: Instrumental activation analysis of standard rocks with high resolution gamma ray detectors. — Geochim. Cosmochim. Acta 32: 369–396.

HANSON, G. N., 1978: The application of trace elements to the petrogenesis of igneous rocks of granitic compositions. — Earth Planet. Sci. Letts. 38: 26–43.

HARRISON, S., 1979: Geology of the major mylonite zone in, and the application of garnet-biotite geothermometry to, the basement rocks of the Olden Window, central Sweden. — Unpubl. B. Sc. thesis, Royal School of Mines, London.

JOHANSSON, L., 1980: Petrochemistry and regional tectonic significance of metabasites in basement windows of the Central Scandinavian Caledonides. — Geol. För. Stockh. Förh. 102: 499–514.

KLINGSPOR, I., and TROËNG, B., 1980: Rb-Sr and K-Ar age determinations of the Proterozoic Olden Granite, central Caledonides, Jämtland, Sweden. — Geol. För. Stockh. Förh. 102: 515–522.

LEROY, J., 1978: The Margnac and Fanay uranium deposits of the La Crouzille District (western Massif Central, France): geologic and fluid inclusion studies. — Econ. Geol. 73: 1611–1634.

LUDWIG, K. R., 1979: A program in Hewlett-Packard BASIC for x-y plotting and line-fitting of isotopic and other data. — U.S. Geol. Survey Open-File 79–1641, 33 pp.

— 1980: Calculation of uncertainties of U-Pb isotope data. — Earth Planet. Sci. Letts. 46: 212–220.

— and SILVER, L. T., 1977: Lead isotope inhomogeneities in Precambrian igneous K-feldspars. — Geochim. Cosmochim. Acta 41: 1457–1471.

LUDWIG, K. R., NASH, J. T., and NAESER, C. W., 1981: U-Pb isotope systematics and age of uranium mineralization Midnite Mine, Washington. — Econ. Geol. 76: 89–110.

LUTH, W. C., JAHNS, R. H., and TUTTLE, O. F., 1964: The granite system at pressures of 4 to 10 kilobars. — J. Geophys. Res. 69: 759–773.

MANTON, W. I., 1973: Whole rock Th-Pb age for the Masuke and Dembe-Divula complexes, Rhodesia. — Earth Planet. Sci. Letts. 19: 83–89.

MASON, P. K., FROST, M. T., and REED, S. J. B., 1969: BM-IC-NPL computer programs for calculating corrections in quantitative X-ray microanalysis. — Nat. Phys. Lab., IMS rep. 2 (unpbl).

MILLARD, H. T., Jr., 1976: Determinations of uranium and thorium in USGS standard rocks by the delayed neutron techniques. — *In* U.S. Geol. Survey Prof. Paper 840: 61–65.

NASH, J. T., 1979: Uranium and thorium in granitic rocks of northeastern Washington and northern Idaho, with comments on uranium resource potential. — U.S. Geol. Survey Open-File Report 79–233, 39 pp.

NKOMO, I. T., STUCKLESS, J. S., THADEN, R. E., and ROSHOLT, J. N., 1978: Petrology and uranium mobility of an early Precambrian granite from the Owl Creek Mountains, Wyoming. — *In* Thirtieth Annual Field Conference-1978 Wyoming Geologic Association Guidebook: 335–348.

— ROSHOLT, J. N., and DOOLEY, J. R., Jr., 1979: U-Th-Pb systematics in surface and drill core samples of a Precambrian basement rock from Laramie, Wyoming. — Earth Sci. Bull. 12, 4: 1–14.

O'NEIL, J. R., and CHAPELL, B. W., 1977: Oxygen and hydrogen isotope relations in the Berridale batholith. — J. Geol. Soc. London 133: 559–571.

— SHAW, S. E., and FLOOD, R. H., 1977: Oxygen and hydrogen isotope compositions as indicators of granite genesis in the New England Batholith, Australia. — Contr. Mineral. Petrol. 62: 313–328.

OVERSBY, V. M., 1975: Isotopic ages and geochemistry of Archaean acid igneous rock for the Pilbara, Western Australia. — Geochim. Cosmochim. Acta 40: 817–829.

PATCHETT, P. J., 1978: Rb/Sr ages of Precambrian dolerites and syenites in southern and central Sweden. — Sver. geol. unders. C 747, 63 pp.

ROGERS, J. J. W., and ADAMS, J. A. S., 1969a: Uranium. — *In* K. H. Wedepohl, ed.: Handbook of geochemistry 2: 4. — Berlin, Springer-Verlag, 92-B to 92-O.

— and ADAMS, J. A. S., 1969b: Thorium. — *In* K. H. Wedepohl, ed.: Handbook of Geochemistry 2: 4. — Berlin, Springer-Verlag, 90-I to 90-O.

ROSHOLT, J. N., ZARTMAN, R. E., and NKOMO, I. T., 1973: Lead isotope systematics and uranium depletion in the Granite Mountains, Wyoming. — Geol. Soc. Amer. Bull. 84: 989–1002.

— and HUESTIS, G. M., 1981: Uranium-series disequilibrium in granite from core samples of drill hole UPH-3, Stephensen County, Illinois. — (Abs.) *in* Geol. Soc. Amer. Abstr. with Programs 13: 541.

SHAND, S. J., 1951: Eruptive rocks. — John Wiley, New York, 488 pp.

SILVER, L. T., 1976: A regional uranium anomaly in the Precambrian basement of the Colorado Plateau (abs.). — Geol. Soc. Amer. Abstr. with Programs 1976, 1107–1108.

SMELLIE, J. A. T., 1982: Radioactive mineral phases from Precambrian granites within the Olden Window, Jämtland, N. Sweden. — Proc. IAEA/OECD Symposium on "Uranium Exploration Methods". Paris, 415—429.

— COGGER, N., and HERRINGTON, J., 1978: Standards for the quantitative determination of uranium and thorium with additional information on the chemical formulae of davidite and euxenite-polycrase. — Chem. Geol. 22: 1–10.

STACEY, J. S., and KRAMERS, J. S., 1975: Approximation of terrestrial lead isotope evolution by a two stage model. — Earth Planet. Sci. Letts. 26: 207–221.

STEIGER, R. H., and JAGER, E., 1977: Subcommission geochronology: Convention on the use of decay constants in geo- and cosmochronology. — Earth Planet. Sci. Letts. 36: 359–362.

STEPHANSSON, O., 1976: A tectonic model of the Offerdal-Olden area, Jämtland. — Geol. För. Stockh. Förh. 98: 112–119.

STRECKEISEN, A. L., 1973: Plutonic rocks, classification and nomenclature recommended by the IUGS subcommission on the systematics of Igneous Rocks. — Geotimes 18: 26–30.

STUCKLESS, J. S., and O'NEIL, J. R., 1973: The petrogenesis of magmas in the Superstition-Superior Volcanic Area, Arizona as inferred from strontium and oxygen isotope data. — Geol. Soc. Amer. Bull. 84: 1987–1998.

— BUNCKER, C. M., BUSH, C. A., DOERING, W. P., and SCOTT, J. H., 1977: Geochemical and petrologic studies of a uraniferous granite from the Granite Mountains, Wyoming. — U.S. Geol. Survey J. Research 5: 61–81.

— and NKOMO, I. T., 1978: Uranium-lead isotope systematics in Uraniferous alkali-rich granites from the Granite Mountains, Wyoming: implications for uranium source rocks. — Econ. Geol. 73: 427–441.

— and VANTRUMP, G., Jr., 1979: A revised version of graphic normative analysis program (GNAP) with examples of petrologic problem solving. — U.S. Geol. Survey Open-File Report 79–1237, 112 pp.

— and NKOMO, I. T., 1980: Preliminary investigations of U-Th-Pb systematics in uranium-bearing minerals from two granitic rocks from the Granite Mountains, Wyoming. — Econ. Geol. 75: 289–295.

— and MIESCH, A. T., 1981: Petrogenetic modeling of a potential uranium source rock, Granite Mountains, Wyoming. — U.S. Geol. Survey Prof. Paper 1225, 34 pp.

— BUNTING, J. A., and NKOMO, I. T., 1981: U-Th-Pb systematics of some granitoids from the northeastern Yilgarn Block, Western Australia and implications for uranium source rock potential.

— J. Geol. Soc. Australia 28, 365—395.

TAGGART, J. E., Jr., LICHTE, F. E., and WAHLBERG, J. S., 1982: Methods of analysis of samples using X-ray fluorescence and induction coupled plasma spectroscopy. — *In* The 1980 eruptions of Mount St. Helen, Washington. — U.S. Geol. Survey Prof. Paper 1250: 683–687.

TATSUMOTO, M., KNIGHT, R. J., and DELEVAUX, M. H., 1972: Uranium, thorium, and lead concentrations in three silicate standards and a method of lead isotopic analysis. — *In* Geological Survey Research 1972. — U.S. Geol. Survey Prof. Paper 800-D: 111–115.

TAYLOR, H. P., Jr., 1968: The oxygen isotope goechemistry of igneous rocks. — Contr. Mineral. Petrol. 19: 1–71.

TAYLOR, S. R., 1964: Abundance of chemical elements in the continental crust: a new table. — Geochem. Cosmochim. Acta 28: 1273–1286.

THORNTON, C. P., and TUTTLE, O. F., 1960: Chemistry of igneous rocks, I. differentiation index. —Amer. J. Sci. 258: 664–684.

TÖRNEBOHM, A. E., 1872: Ueber die Geognosie Schwedischen Hochgebirge. — Bihang till Kongl. Svenska Vetenskapsakademien 1: 1–60.

— 1896: Grunddragen av det centrala Skandinaviens bergbyggnad. — Kongl. Svenska Vetenskapsakademiens Handlingar 28, 212 pp.

TROËNG, B., 1982: Uranium rich granites in the Olden Window, Sweden. — Min. Mag. 46: 219–228.

— and WILSON, M. R., 1982: Geological setting of uranium mineralizations in the Hotagen area; central Swedish Caledonides. — *In:* Vein-type and Similar Uranium Deposits in Rocks Younger than Proterozoic. — Proc. Tech. Comm. Meeting, Lisbon, IAEA, Vienna, 65—85.

TUTTLE, O. F., and BOWEN, N. L., 1958: Origin of granites in the light of experimental studies in the system $NaAlSi_3O_8$-$KAlSi_3O_8$-$CaAl_2Si_2O_8$. — Geol. Soc. Amer. Mem. 74, 153 pp.

WALSER, G., 1980: Geology of the Hotagen area, Jämtland, Central Sweden. — Sver. geol. unders. C 757: 1–25.

WENNER, D. B., 1981: Oxygen isotopic compositions of the late orogenic granites in the southern Piedmont of the Appalachian Mountains, USA, and their relationship to subcrustal structures and lithologies. — Earth Planet. Sci. Letts. 54: 186–199.

WHITNEY, J. A., 1975: The effects of pressure, temperature and X_{H_2O} on phase assemblages in four synthetic rock compositions. —J. Geol. 83: 1–27.

WILSON, M. R., and SUNDIN, N. O., 1979: Isotopic age determinations on rocks and minerals from Sweden 1960–1978. — Sver. geol. unders., Rapp. och medd. 16, 41 pp.

YORK, D., 1969: Least-squares fitting of a straight line with correlated errors. — Earth Planet. Sci. Letts. 5: 320–324.

ZIELINSKI, R. A., 1975: Trace element evolution of a suite of rocks from Reunion Island, Indian Ocean. — Geochim. Coshmochim. Acta 39: 713–734.

— PETERMAN, Z. E., STUCKLESS, J. S., ROSHOLT, J. N., and NKOMO, I. T., 1981: The chemical and isotopic record of rock-water interaction in the Sherman Granite, Wyoming and Colorado. — Contr. Mineral. Petrol. 78: 209–219.

APPENDIX

Description of samples from the Olden Window, Sweden

76032 — Surface sample. Coarse-grained, porphyritic granite with some chloritized primary biotites and mobilized secondary biotite associated with epidote and muscovite. Accessory and secondary minerals include zircon, fluorite, sphene, and allanite.

76285 — Surface sample. Fine-grained, porphyritic gneissic granite rich in biotite and showing chloritization.

77660 — Drill-core samples from 57.0 m depth. Coarse-grained, cataclastically deformed granite with minor mineralization and extensive mobilization of biotite. Accessory and secondary minerals include muscovite, zircon, sphene, and allanite. (Drill-core: 78014.)

77662 — Drill-core sample from 58.5 m depth. Coarse-grained, cataclastically deformed to brecciated and biotite infilled granite. Accessory and secondary minerals include muscovite, zircon, epidote, sphene, ilmenite, pitchblende, and altered pitchblende or coffinite. (Drill-core: 78014.)

77666 — Drill-core sample from 60.0 m depth. Coarse-grained, cataclastically deformed granite with minor mineralization and some mobilization of biotite. Accessory and secondary minerals include zircon, sphene, allanite, and muscovite. (Drill-core: 78014.)

77735 — Drill-core sample from 97.0 m depth. Medium- to coarse-grained, cataclastically deformed granite. A portion of the sample exhibits biotitic alteration and mineralization. Secondary and accessory minerals include muscovite, fluorite, epidote, chlorite, allanite, zircon, sphene, ilmenite, pyrite, uranothorite, pitchblende, and a uranosilicate. (Drill-core: 78017.)

77738 — Drill-core samples from 99 m depth. Coarse-grained, cataclastically deformed and brecciated granite with strong biotitic alteration and mineralization. Secondary and accessory minerals include muscovite, epidote, sphene, zircon, pitchblende, fluorite, and secondary uranium minerals. (Drill-core: 78017.)

77968 — Drill-core sample from 1.5 m depth. Coarse-grained, cataclastically deformed granite with some biotitic alteration. Secondary and accessory minerals include muscovite, chlorite, zircon, magnetite, allanite, sphene, and monazite-cheralite. (Drill-core: 78017.)

77972 — Drill-core sample from 64.0 m depth. Medium- to coarse-grained, cataclastically deformed granite. Secondary and accessory minerals include muscovite, sphene, fluorite, chlorite, allanite, pyrite, and uranothorite. (Drill-core: 78017.)

77979 — Drill-core sample from 155.0 m. Coarse-grained, cataclastically deformed granite. Secondary and accessory minerals include muscovite, chlorite, sphene, allanite, ilmenite, and zircon. (Drill-core: 78017.)

77981 — Drill-core sample from 0.6 m depth. Medium- to coarse-grained granite. Sample is somewhat less deformed and more mafic than most samples from Lilljuthatten. Secondary and accessory minerals include muscovite, magnetite, chlorite, zircon, sphene, epidote, ilmenite, and fluorite. The latter is enclosed in plagioclase and apparently primary. (Drill-core: 78014.)

77988 — Drill-core sample from 120.7 m depth. Coarse-grained granite with slight cataclastic deformation. Secondary and accessory minerals include muscovite, allanite, zircon, and ilmenite. (Drill-core: 78014.)

79061 — Surface sample. Fine- to medium-grained, cataclastically deformed, leucocratic granite. Secondary and accessory minerals include muscovite, chlorite, zircon, and magnetite. (Co-ordinates: 7098220 1401670.)

79062 — Surface sample. Medium- to coarse-grained, cataclastically deformed granite. Secondary and accessory minerals include muscovite, chlorite, magnetite, and ilmenite. (Co-ordinates: 7098430 1402470.)

79070 — Surface sample. Coarse-grained biotite granite with minor cataclastic deformation. Secondary minerals include chlorite, allanite, sphene, zircon, and fluorite. (Co-ordinates: 7097030 1405180.)

79901 — Drill-core sample from 106.3 m depth. Medium-grained, cataclastically deformed biotite granite. Secondary and accessory minerals include muscovite, zircon, allanite, fluorite, and magnetite. (Drill-core: 77001.)

79903 — Drill-core sample from 184.1 m depth. Coarse-grained, cataclastically deformed, leucocratic granite. This sample is the only one that exhibits reaction textures between plagioclase and potassium feldspar. Secondary and accessory minerals include zircon, ilmenite, allanite, and fluorite. (Drill-core: 77001.)

79906 — Drill-core sample from 197.3 m depth. Coarse-grained, cataclastically deformed granite. Secondary and accessory minerals include muscovite, allanite, zircon, chlorite, and ilmenite. (Drill-core: 77001.)

79908 — Drill-core sample from 5.7 m depth. Medium- to coarse-grained, cataclastically deformed granite. Secondary and accessory minerals include muscovite, allanite, zircon, fluorite, chlorite, and relatively abundant magnetite. (Drill-core: 77002.)

79911 — Drill-core sample from 76.5 m depth. Coarse-grained, cataclastically deformed granite. Potassium feldspar and sphene are notably abundant. Sample exhibits mineralization and biotite infilling. Secondary and accessory minerals include muscovite, sphene, pitchblende, and ilmenite. (Drill-core: 77002.)

79912 — Drill-core sample from 113.0 m depth. Coarse-grained, cataclastically deformed and biotitically altered granite. Quartz content is markedly depleted. Secondary and accessory minerals include muscovite, chlorite, sphene, allanite, zircon, and magnetite. (Drill-core: 77002.)

79914 — Drill-core sample from 129.5 m depth. Medium- to coarse-grained, cataclastically deformed biotite granite. Secondary and accessory minerals include muscovite, chlorite, epidote, allanite, ilmenite, zircon, and fluorite. (Drill-core: 77002.)

79917 — Drill-core sample from 140.1 m depth. Coarse-grained, cataclastically deformed and brecciated granite with much biotite infilling. Secondary and accessory minerals include muscovite, sphene, magnetite, and zircon. (Drill-core: 78007.)

Lill-1 — Surface sample. Coarse-grained, cataclastically and plastically deformed granite. Secondary and accessory minerals include muscovite, chlorite, zircon, magnetite, and fluorite.

78023 — Surface sample. Vein of galena within the metavolcanic rocks in a structure that is parallel to Caledonian structures.

78026 — Surface sample. Vein of galena, quartz and fluorite that cuts microgranite close to the nappes in the western part of the window.

78240 — Surface sample. Quartz and galena replacement vein in the microgranite south of Lilljuthatten.

78313 — Surface sample. Quartz, galena, sphalerite, and chalcopyrite vein that cuts the microgranite and parallels Caledonian structures. (Co-ordinates: 7078196 1385498.)

PRISKLASS D

Distribution
Liber Kartor
162 89 STOCKHOLM

ISBN 91-7158-277-0
ISSN 0082-0024

Schmidts Boktryckeri AB
Helsingborg 1982